Quantum Billiards, Microwave Billiards and Quantum Graphs

Microwave billiard

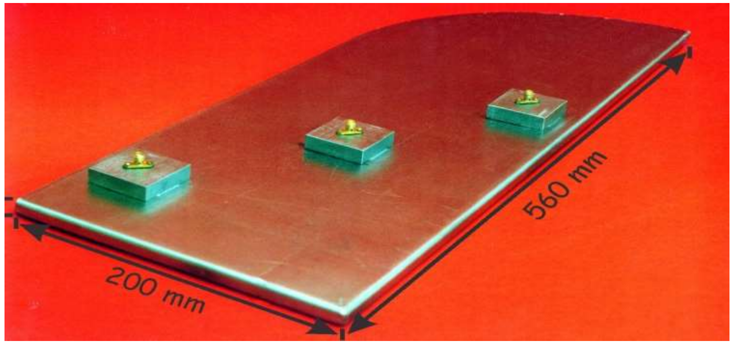

Quantum Graph

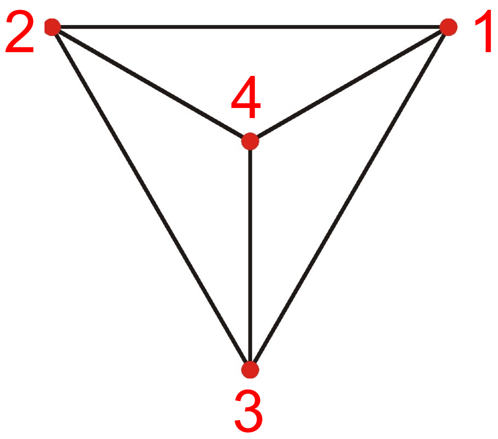

Microwave Network

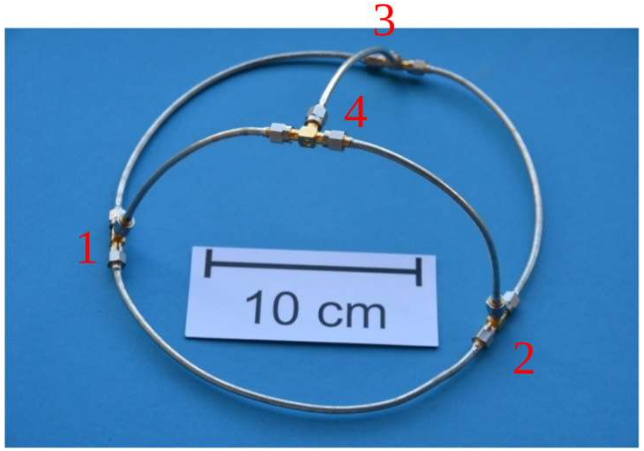

From: Quantum Chaos Group
TU Darmstadt
Achim Richter, BD

From: Quantum Gaph Group
Polish Academy of Science
Warsaw
Leszek Sirko

Classical Billiard

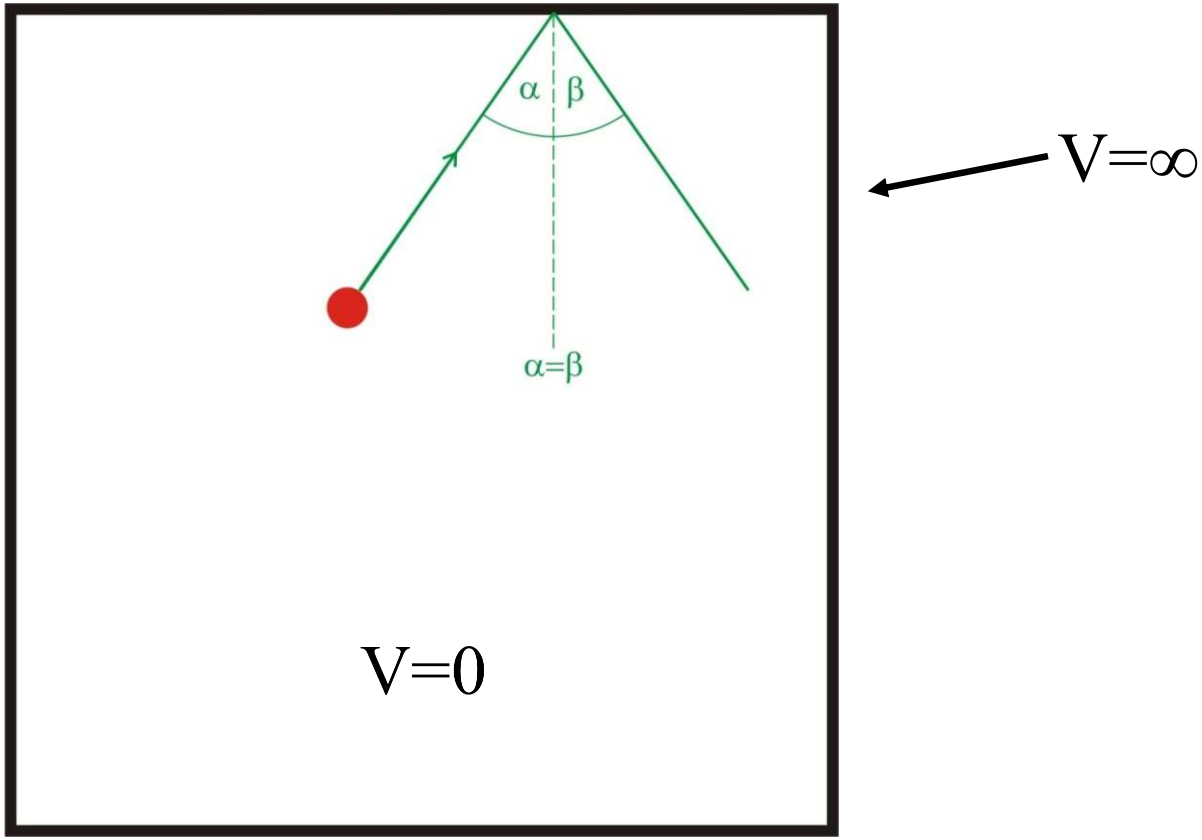

- Particle moves freely within the billiard along straight lines with constant velocity and is reflected specularly at boundary
- Shape of billiard determines chaoticity of classical dynamics

Quantum Billiards and Microwave Billiards

- Experimental determination of the eigenvalues and wave functions of the quantum billiard with microwave billiards

Quantum billiard

Microwave billiard

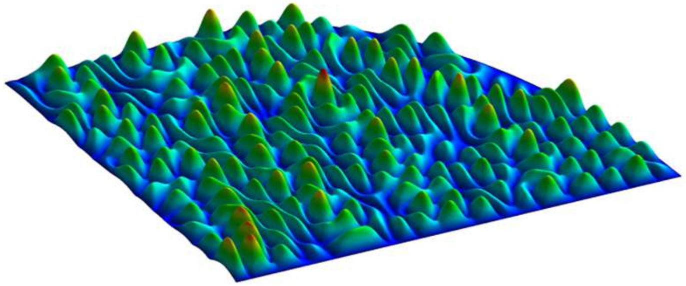

$\longleftrightarrow$

$f < f_{max} = c/2h$

$k = \frac{2\pi f}{c}$

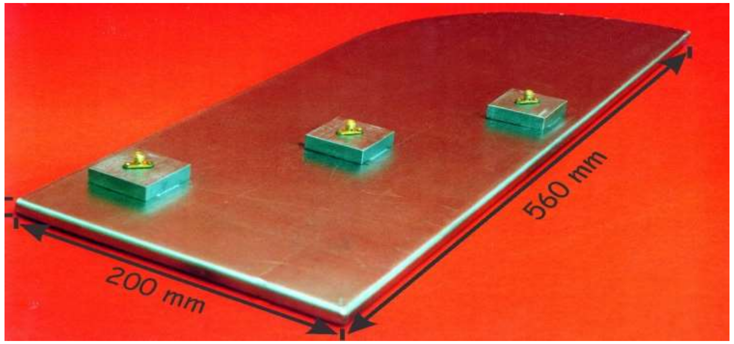

$$\left(\frac{\hbar^2}{2m}\Delta + E\right)\Psi = 0, \quad \Psi\big|_{\partial\Omega} = 0$$

$$\left(\Delta + k^2\right) E_z = 0, \;\; E_z\big|_{\partial\Omega} = 0$$

eigenvalue E $\leftrightarrow$ resonance frequency f

eigenfunction Ψ $\leftrightarrow$ electric field strength E_z

Measurement Principle

- Measurement of the scattering matrix element S_{21} with a superconducting cavity

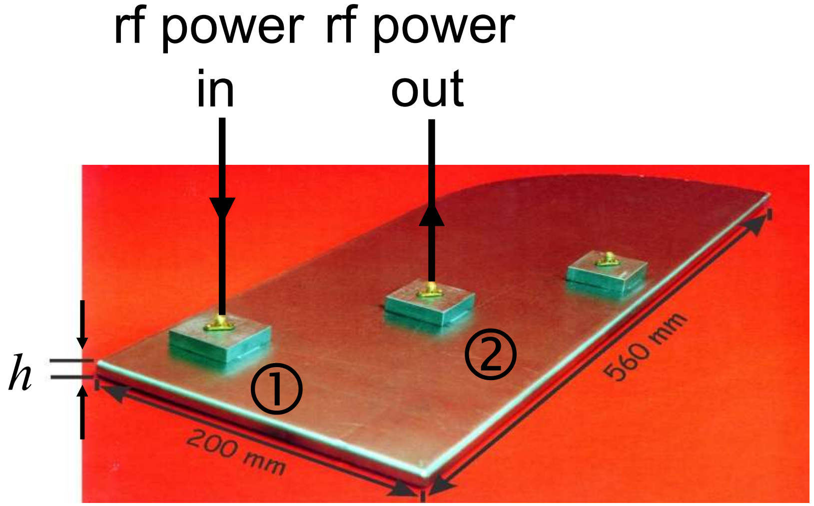

$$\longrightarrow \quad \frac{P_{out,2}}{P_{in,1}} = \left|S_{21}\right|^2$$

Resonance spectrum

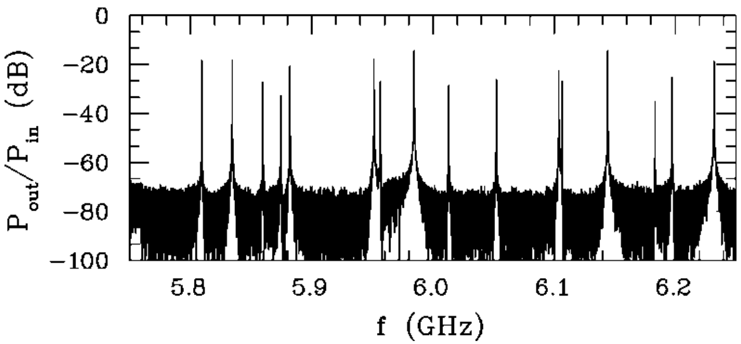

$\longrightarrow$ positions of the resonances $f_n = k_n c/2\pi$ yield eigenvalues

Unfolding of Spectra

- Integrated spectral density $N(E)$ = # levels below E

- Decompose into a smooth and a fluctuating part

$$N(E) = \overline{N}(E) + N^{fluc}(E)$$

- Replace eigenvalues E_{i} by the smooth part of the integrated spectral density

$$e_i = \overline{N}(E_i)$$

- Quantum billiard / Microwave billiard:

Weyl formula: $\overline{N}\left(k=\sqrt{E}\right) = N^{Weyl}(k) = \frac{A}{4\pi}k^2 - \frac{U}{4\pi}k + const.$

Indispensable Requirements on Analysis of Fluctuation Properties

- Completeness of the level sequences. Missing levels imply changes in the fluctuation properties
- Unambiguous assignment of the states to the relevant symmetry classes like, e.g., spin J and parity π in nuclei, or geometric symmetries in quantum billiards
- Either needs level sequences with similar fluctuation properties containing at least 5 levels in an ensemble of many nuclei or a complete sequence of at least ~100 levels in one nucleus / one quantum billiards

Complete Identification of States in ^{208}Pb Below 6.20 MeV

A. Heusler et al., Phys. Rev. C 93, 054321 (2016)

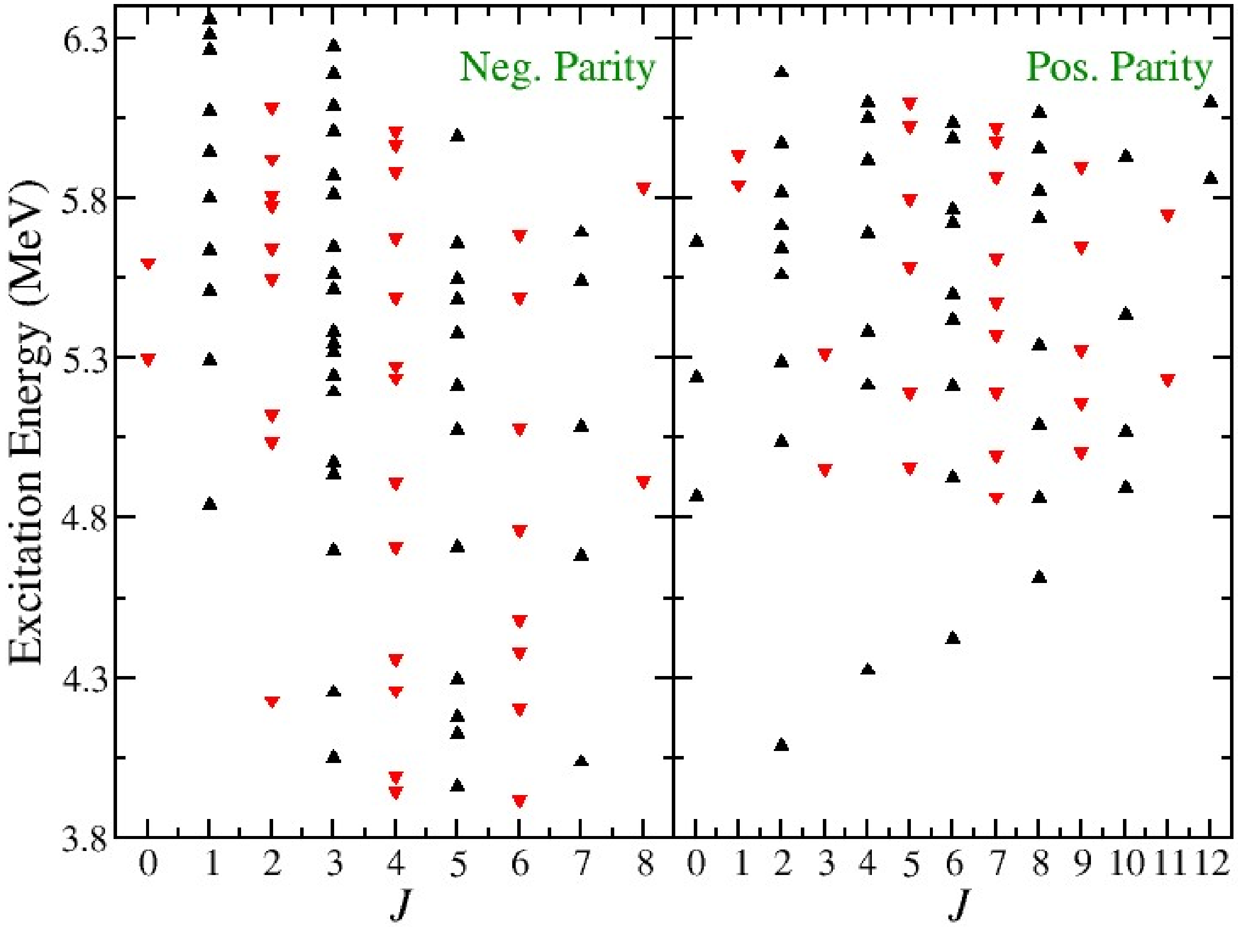

- Below 6.20 MeV a complete sequence of 151 levels was identified
- For each state, spin J and parity π were determined unambiguously

Fluctuating Part of the Integrated Spectral Density of the Complete Sequence

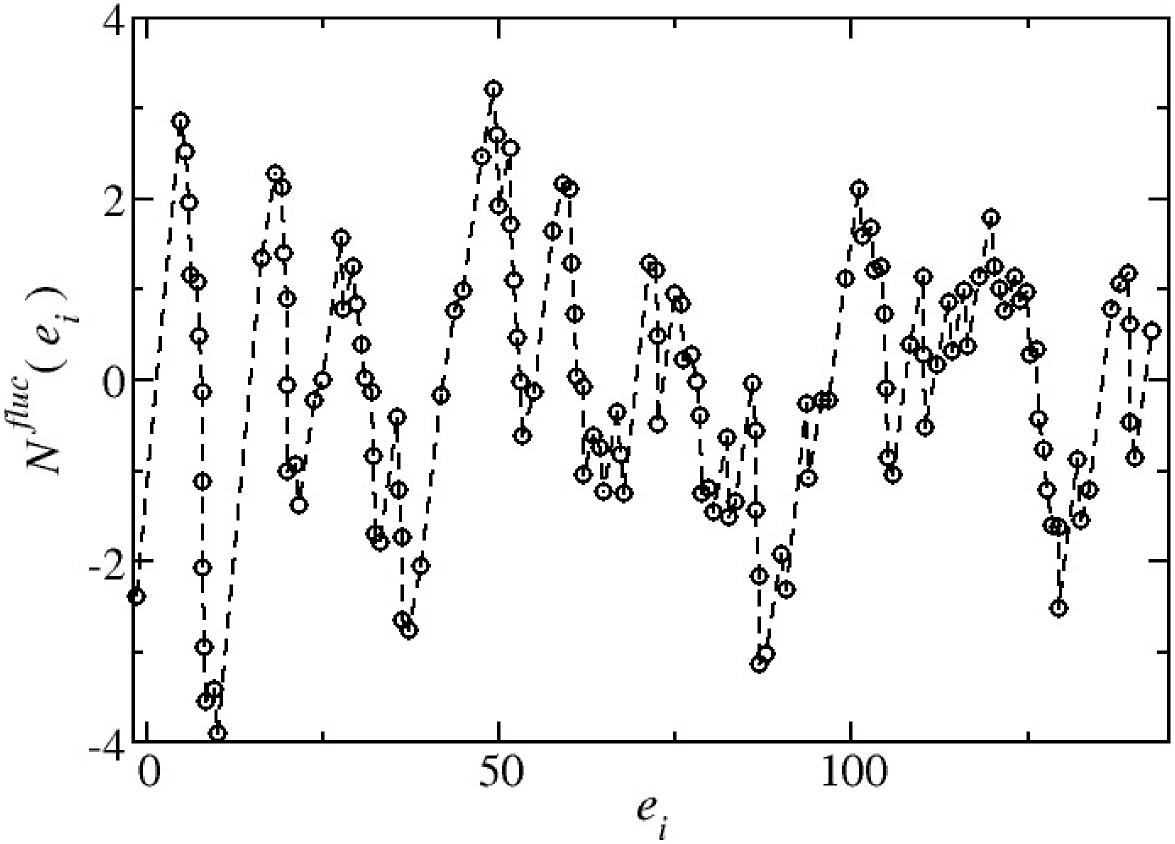

- All 151 energy levels irrespective of their spin and parity were used
- N^{fluc} fluctuates around zero $\rightarrow$ clear indication that spectrum is complete

Spectral Properties of the Complete Sequence

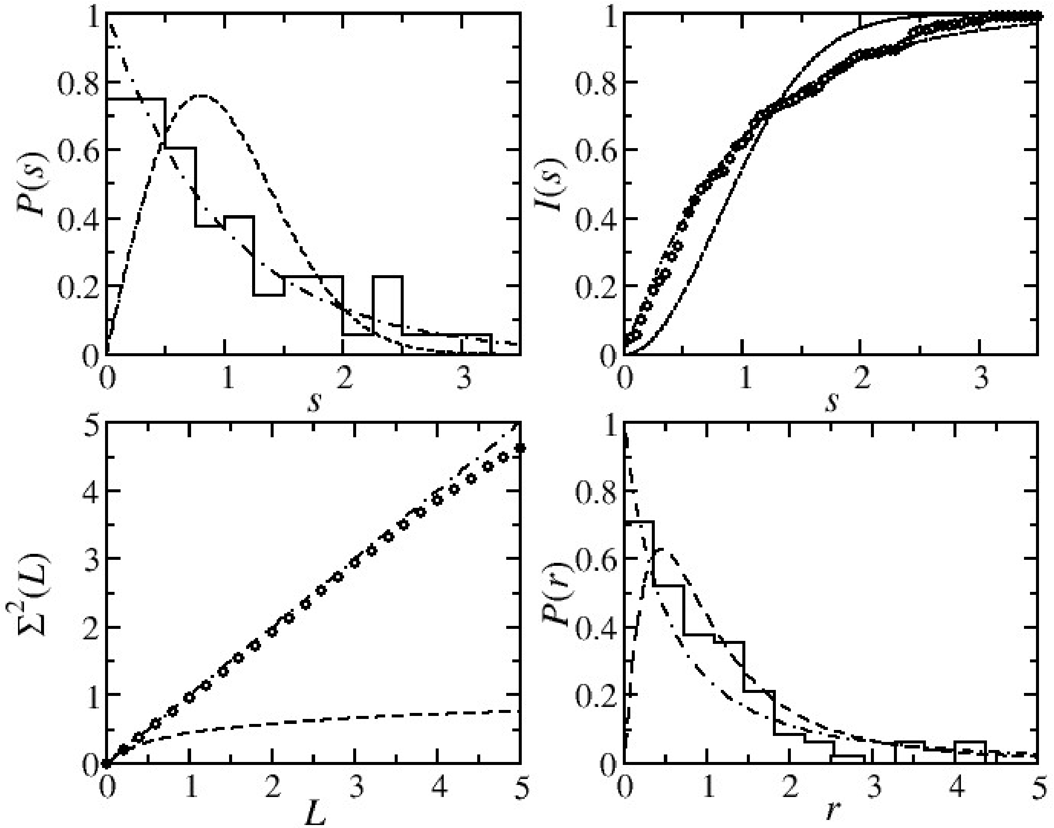

- Spectral properties agree with those of random Poissonian numbers
- Reason: Superposition of states belonging to different symmetry classes
- In order to attain information on the underlying nucleon dynamics, the spectra need to be separated into subspectra characterized by J^{π}

Ensemble Averages of Symmetry-Projected States

Dietz et al., PRL 118, 012501 (2017)

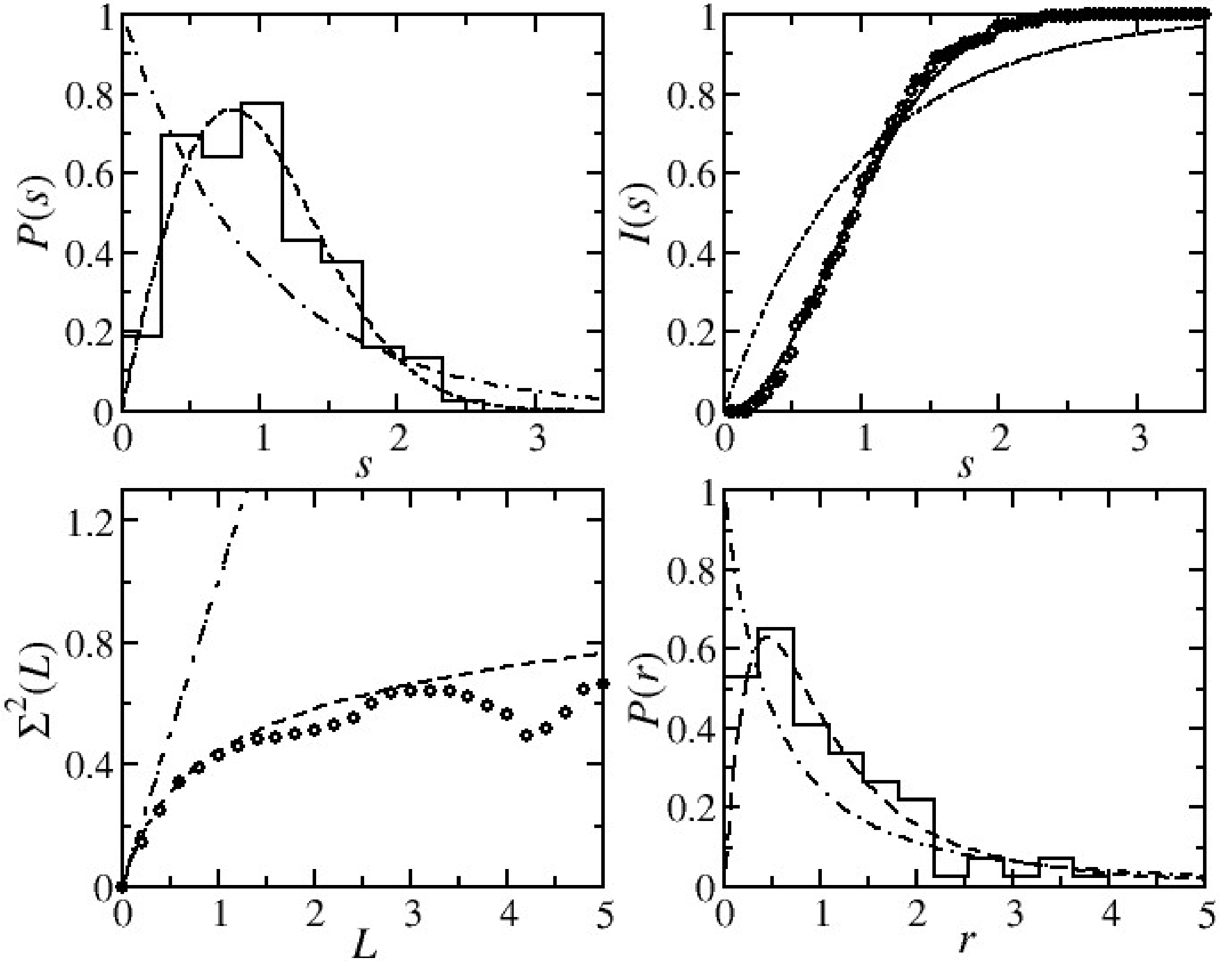

- The spectral properties of the ensemble agree well with those of random matrices from the GOE, thus indicating chaoticity of the nuclear system

Mirror Symmetries

Eigenvalues: $E(m,n) = \frac{\pi^2}{8}\left[\frac{m^2}{a^2} + \frac{n^2}{b^2}\right]$

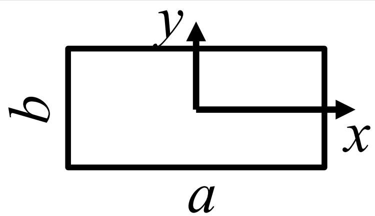

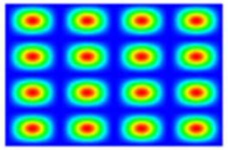

Dirichlet-Dirichlet

$\psi = 0$ at x & y axes

$$\Psi_{m,n}(x,y) = A \sin\left(\frac{m\pi x}{2a}\right) \sin\left(\frac{n\pi y}{2b}\right),$$

m even, n even,

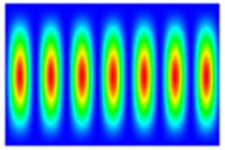

Neumann-Neumann

$\partial_n \psi = 0$ at x & y axes

$$\Psi_{m,n}(x,y) = A \cos\left(\frac{m\pi x}{2a}\right) \cos\left(\frac{n\pi y}{2b}\right),$$

m odd, n odd,

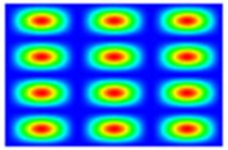

Dirichlet-Neumann

$$\Psi_{m,n}(x,y) = A \sin\left(\frac{m\pi x}{2a}\right) \cos\left(\frac{n\pi y}{2b}\right),$$

m even, n odd,

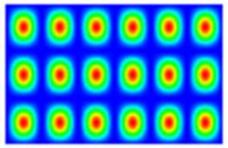

Neumann-Dirichlet

$$\Psi_{m,n}(x,y) = A \cos\left(\frac{m\pi x}{2a}\right) \sin\left(\frac{n\pi y}{2b}\right),$$

m odd, n even,

Nonrelativistic QBs with a Discrete Rotational Symmetry

- Billiard domain in polar coordinates

$$\boldsymbol{r} = [x(r,\varphi), y(r,\varphi)],\ w(r,\varphi) = x(r,\varphi) + iy(r,\varphi),\ \varphi \in [0, 2\pi),\ r \in [0, r_0]$$

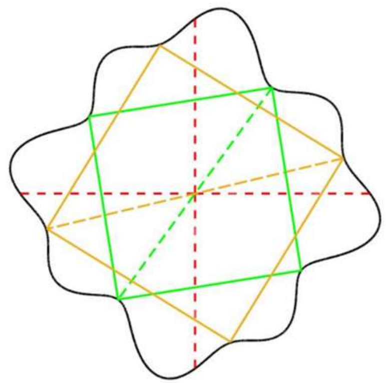

- M-fold rotational symmetry: $w\left(\varphi + \lambda\frac{2\pi}{M}\right) = e^{i\lambda\frac{2\pi}{M}} w(\varphi)$

- Schrödinger equation of the QB with Dirichlet BC

$$\hat{H}\psi_m(r,\varphi) = -\Delta_{(r,\varphi)}\psi_m(r,\varphi) = k_m^2\psi_m(r,\varphi) \quad \text{with} \quad \psi_m(r,\varphi)|_{r=r_0} = 0.$$

- Rotation by $2\pi/M$: $\hat{R} = e^{i\frac{2\pi}{M}\hat{L}}$

- Wave functions classifiable according to their transformation properties

$$\hat{R}^\lambda\psi_m^{(l)}(r,\varphi) = \psi_m^{(l)}\left(r, \varphi - \frac{2\pi}{M}\lambda\right) = e^{il\frac{2\pi}{M}\lambda}\psi_m^{(l)}(r,\varphi) \qquad l,\lambda = 0,1,2,..,M\text{-}1$$

- Apply time-reversal operator $\hat{T} = \hat{C}$

$$\hat{C}\psi_m^{(l)}\left(r, \varphi - \frac{2\pi}{M}\lambda\right) = e^{i(M-l)\frac{2\pi}{M}\lambda}\left[\psi_m^{(l)}(r,\varphi)\right]^* \quad \overset{\text{T invariance}}{\Rightarrow} \quad \left[\psi_m^{(l)}(r,\varphi)\right]^* = \psi_m^{(M-l)}(r,\varphi).$$

- Eigenvalues of states with l, M-l with $l \neq 0, M/2$ are degenerate

Symmetry-Projected Boundary Integral Equations for QBs

- Boundary-integral equation can be written in the form

$$u(\varphi') = \int_0^{2\pi} d\varphi |w'(\varphi)| Q^{QB}(k;\varphi,\varphi') u(\varphi) \quad \text{with} \quad u(\phi) = \partial_n \psi(\phi)$$

$$Q^{QB}(k;\varphi,\varphi') = i\frac{k}{2}\cos\left[\alpha(\varphi') - \xi(\varphi,\varphi')\right] H_1^{(1)}(k\rho)$$

$$e^{i\xi(\varphi,\varphi')} = \frac{w(\varphi) - w(\varphi')}{|w(\varphi) - w(\varphi')|},\ \rho(\varphi,\varphi') = |w(\varphi) - w(\varphi')|$$

- M-fold symmetry $\qquad w\left(\varphi + \lambda\frac{2\pi}{M}\right) = e^{i\lambda\frac{2\pi}{M}} w(\varphi)$

- Symmetry-projected boundary-integral equations

$$u^{(l)}(\varphi') = \int_0^{\frac{2\pi}{M}} d\varphi \tilde{Q}^{(l)}(k;\varphi,\varphi') u^{(l)}(\varphi)$$

$$\tilde{M}_\lambda(k;\varphi,\varphi') = \tilde{Q}\left(k;\varphi + \lambda\frac{2\pi}{M},\varphi'\right) \quad \tilde{Q}^{(l)}(k;\varphi,\varphi') = \sum_{\lambda=0}^{M-1} e^{i\frac{2l\pi}{M}\lambda} \tilde{M}_\lambda(k;\varphi,\varphi') \qquad \tilde{Q} = Q^{QB}$$

Spectral Properties of the 4Fold-symmetric QB and its Symmetry-Projected Eigenstates

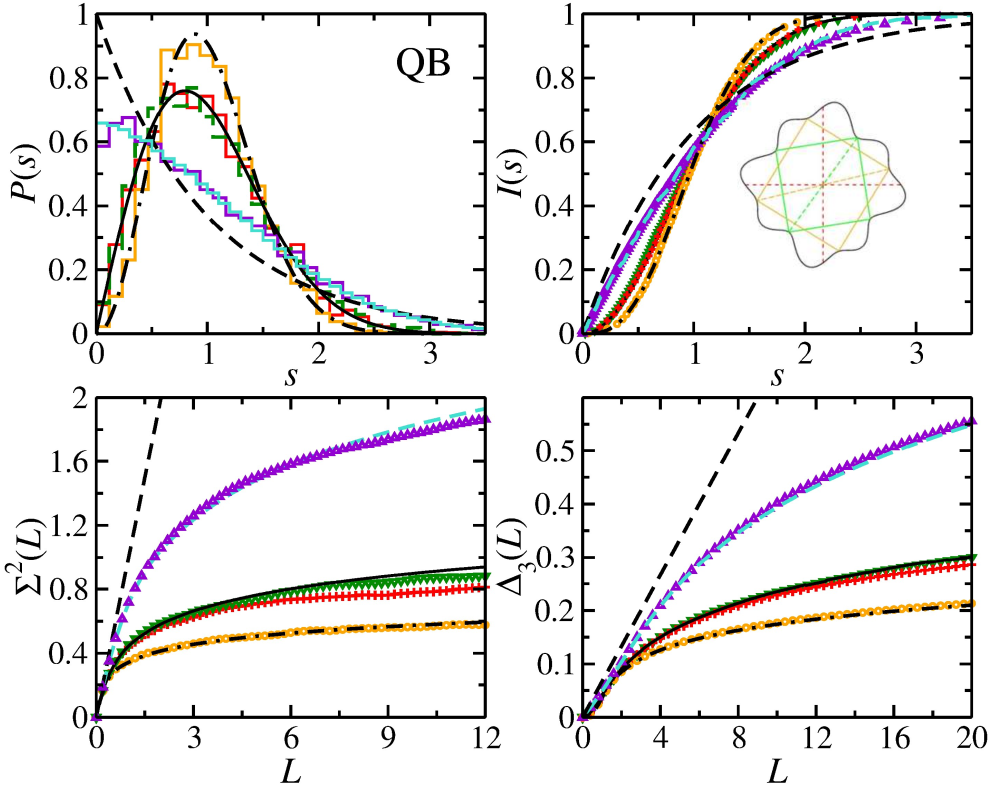

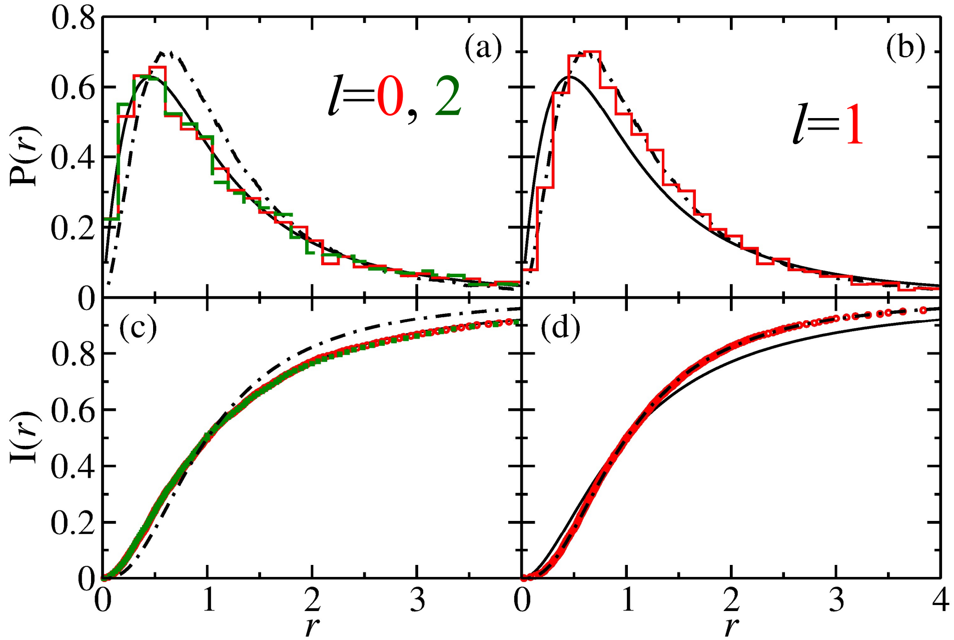

- Spectral properties of all levels (violet) agree with 2GOE+1GUE (turquoise)
- The spectral properties of the symmetry-projected eigenstates with l=0, l=2 agree with GOE, those of l=1, l=3 are degenerate and agree with GUE

→ Does not comply with BGS because the billiard system is T invariant

Length Spectra of the 4Fold-symmetric QB and its Symmetry-Projected Eigenstates

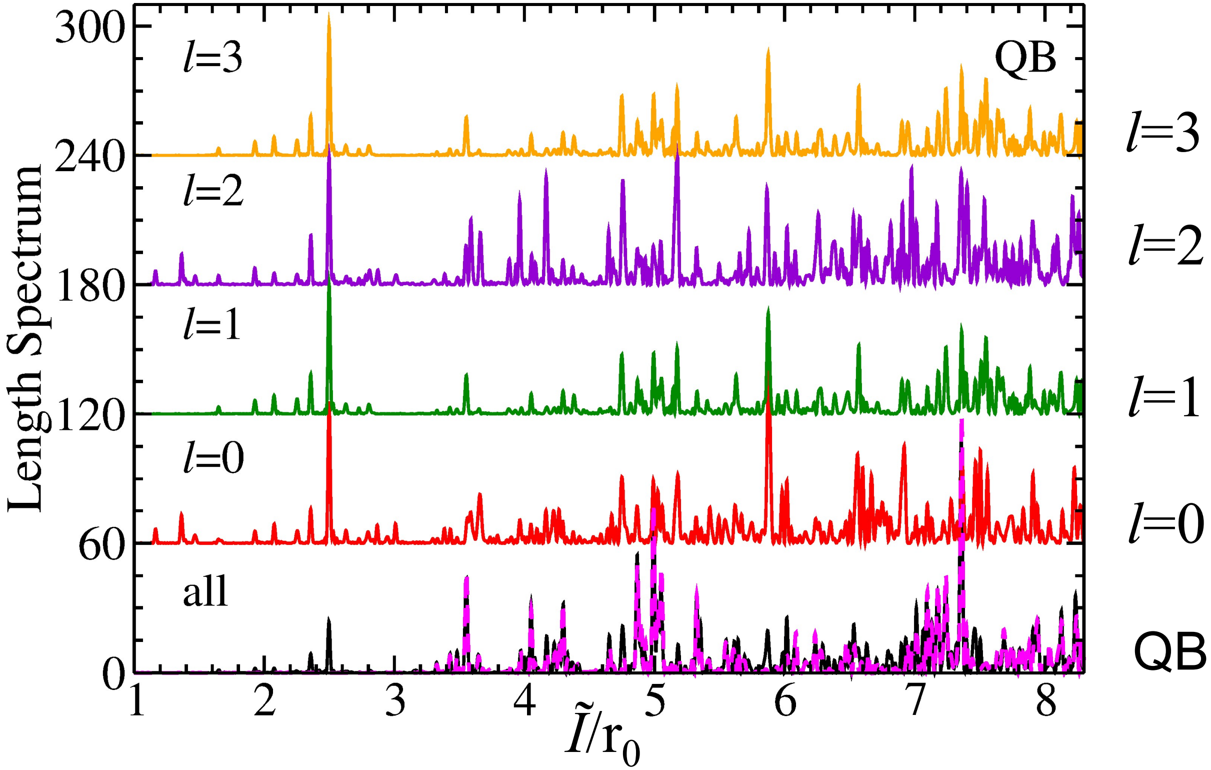

- For the symmetry-projected cases peaks appear at lengths of pseudo orbits
- Magenta: Obtained by summing over the complex-valued Fourier transforms for all symmetry classes
- Black: Obtained from the eigenvalues for $l=0,1,2 \Rightarrow$ below $\tilde{l}/r_0=3$ there are only pseudo orbits

Constant Width Billiards

O. Knill, Elemente der Mathematik 53, 89 (1998)

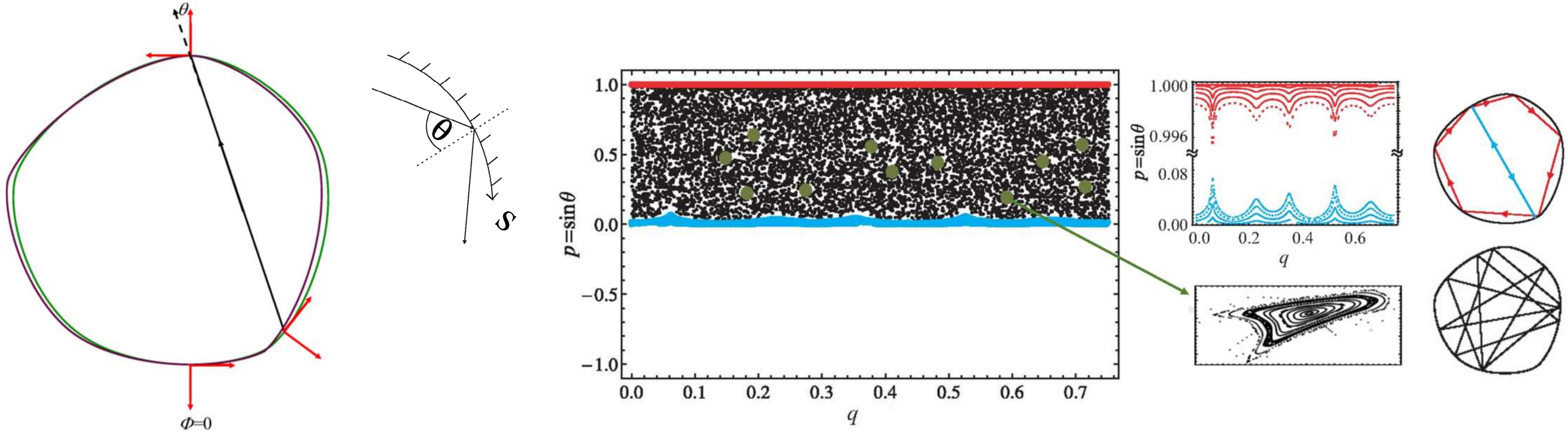

- Classical dynamics is unidirectional
- Change from clockwise to anti-clockwise motion classically forbidden
- In quantum billiard transition from $p>0$ to $p<0$ possible due to tunneling

$$w(\phi) = -R_0 i e^{i\phi} - i a_3 \left[\frac{(e^{i4\phi}-1)}{4} + \frac{(e^{-i2\phi}-1)}{2}\right] - i a_5 \left[\frac{(e^{i6\phi}-1)}{6} - \frac{(e^{-i4\phi}-1)}{4}\right],\ \phi \in [0, 2\pi)$$

$$w'(\phi) = \mathcal{R}(\phi) e^{i\phi},\ \mathcal{R}(\phi) = R_0 + 2 i a_3 \sin(3\phi) + 2 a_5 \cos(5\phi),\ \mathcal{R}(\phi) = \mathcal{R}^*(\phi)$$

$$\boldsymbol{t}(\phi) = [\cos\phi, \sin\phi] \qquad \boldsymbol{n}(\phi) = \left[\cos\left(\phi - \tfrac{\pi}{2}\right), \sin\left(\phi - \tfrac{\pi}{2}\right)\right]$$

Constant Width Microwave Billiard
Dietz et al., PRE 90, 022903 (2014)

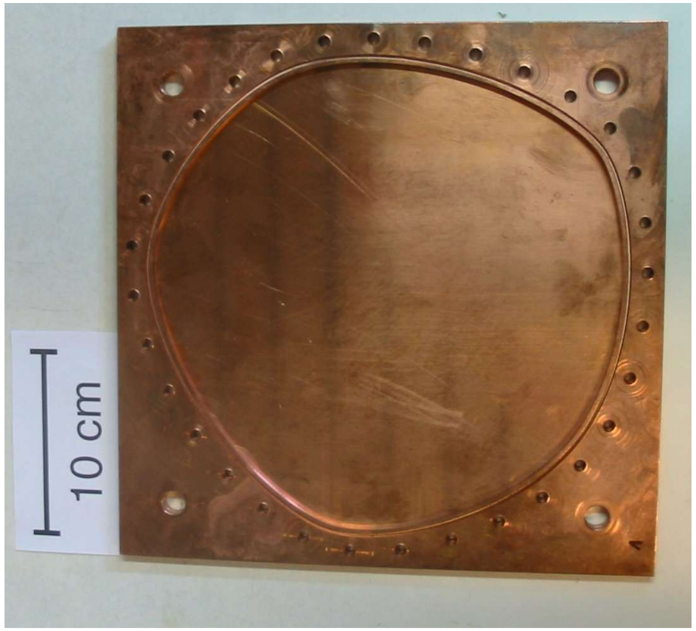

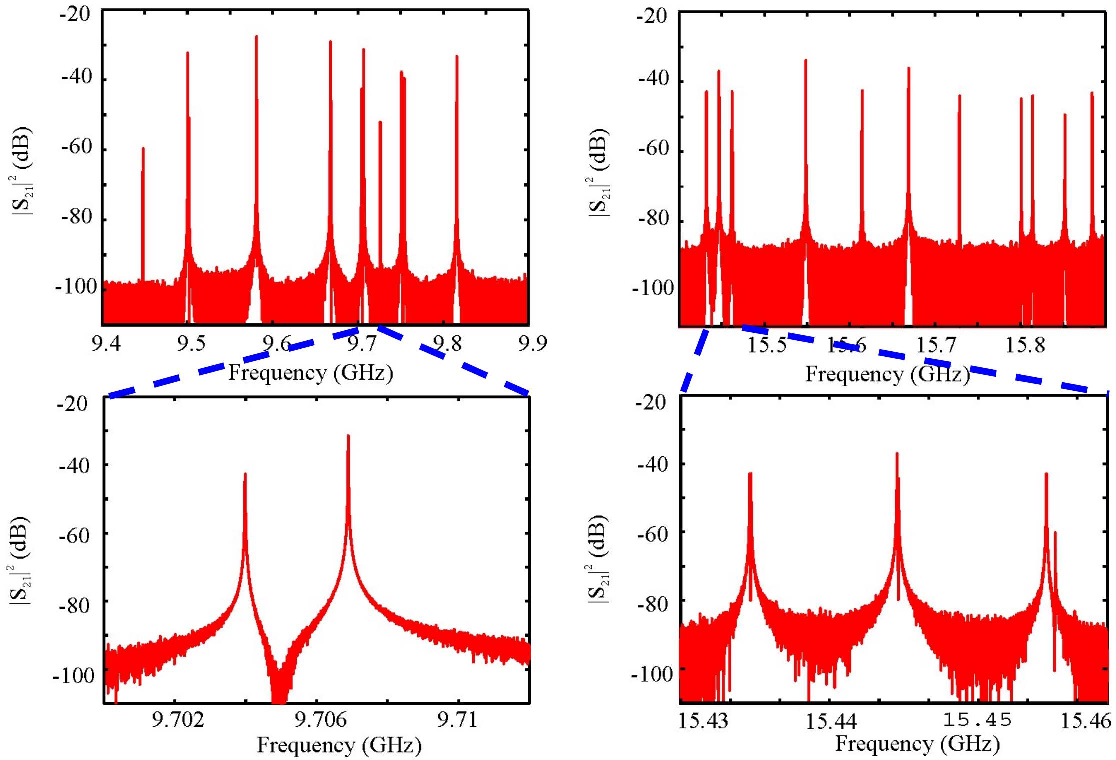

- Construction of two superconducting microwave billiards ($Q=10^6$)
- Degenerate resonances are split into doublets due to tunneling
- Singlets correspond to diameter orbit ($p=0$). The sequence of doublets can be split into two independent spectra $\{k_n^l\}, \{k_n^r\}$

Wave function and Husimi function of a Singlet Mode

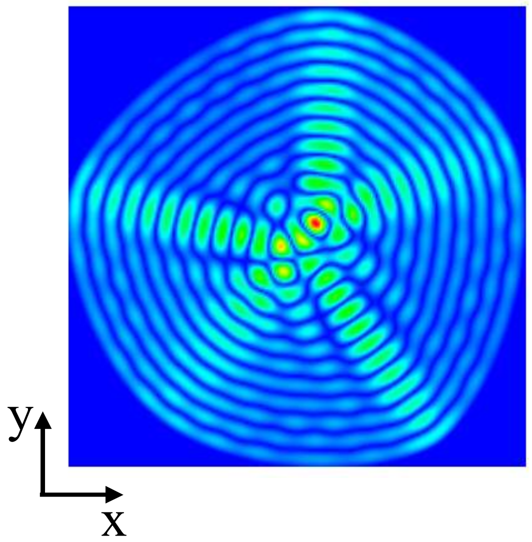

Quantum PSOS

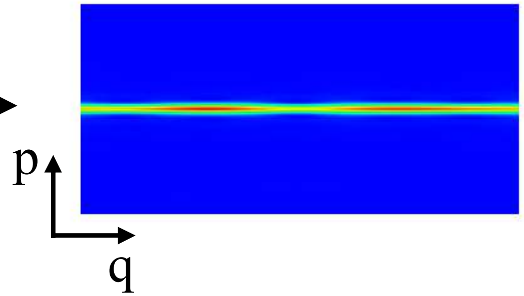

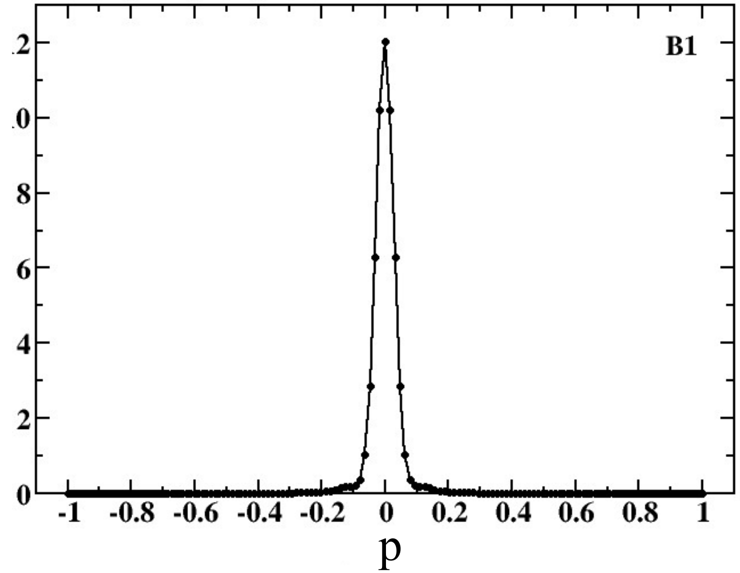

- Wave function looks like a deformed J_0-eigenfunction of circle billiard
- Husimi function on PSOS: Projection of boundary function onto a coherent state on the billiard boundary, $C^{\sigma}_{(p,q)}(s;k_n)$

$$H_n(p,q) = \frac{1}{2\pi k_n} \frac{1}{\int_0^L \mathrm{d}s \left| \left\langle \hat{n}(s), \vec{\nabla}\Psi_n(s) \right\rangle \right|^2} \left| \int_0^L \mathrm{d}s \left\langle \hat{n}(s), \vec{\nabla}\Psi_n(s) \right\rangle C^{\sigma}_{(p,q)}(s;k_n) \right|^2$$

QB: Modes Localized on and Around Diameter Orbit

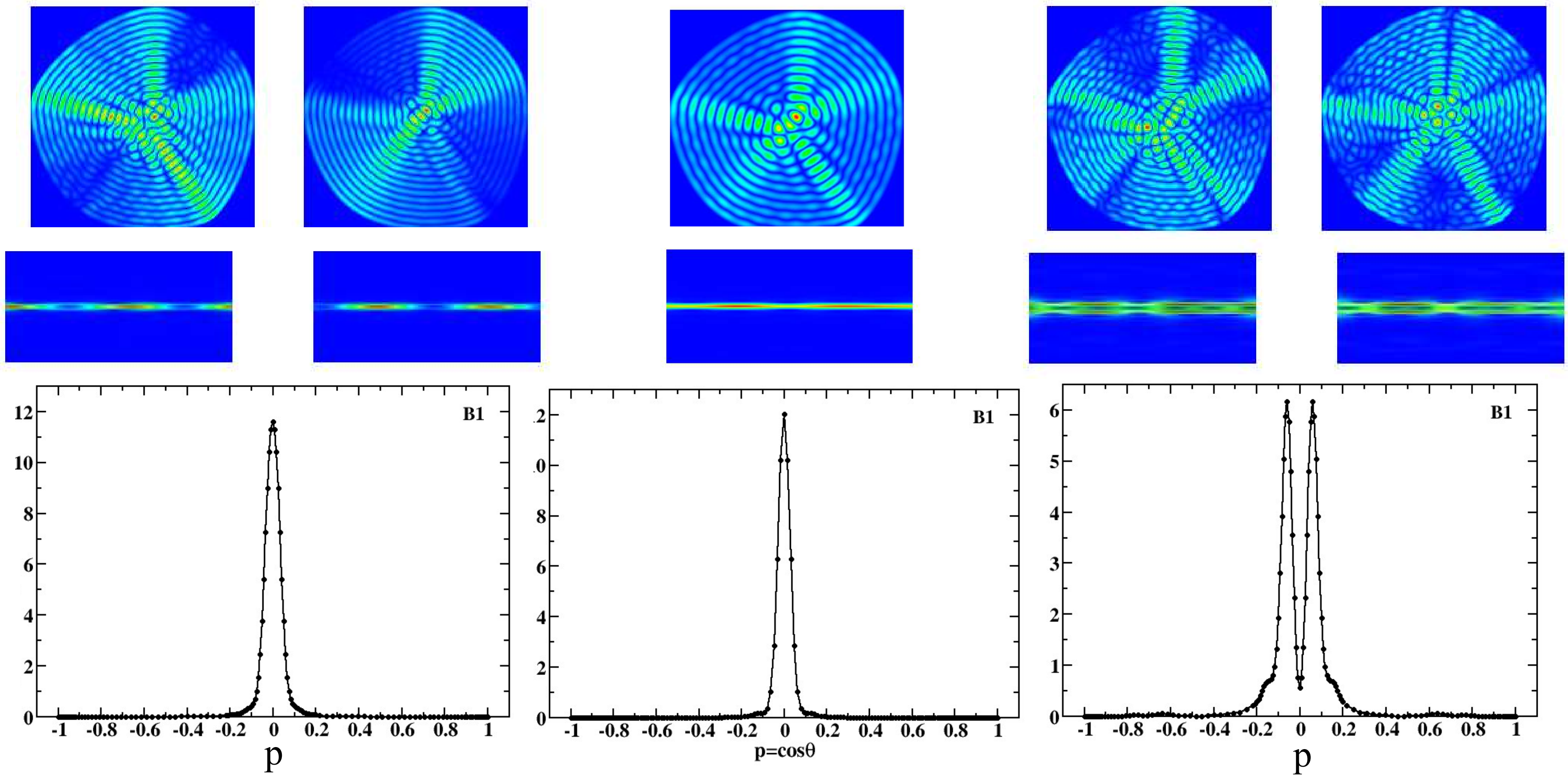

‘Symmetric DO’ has maximum at $p=0$ ‘Asymmetric DO’ has minimum at $p=0$

QB: Whispering Gallery Modes and Modes Associated with Regular Island

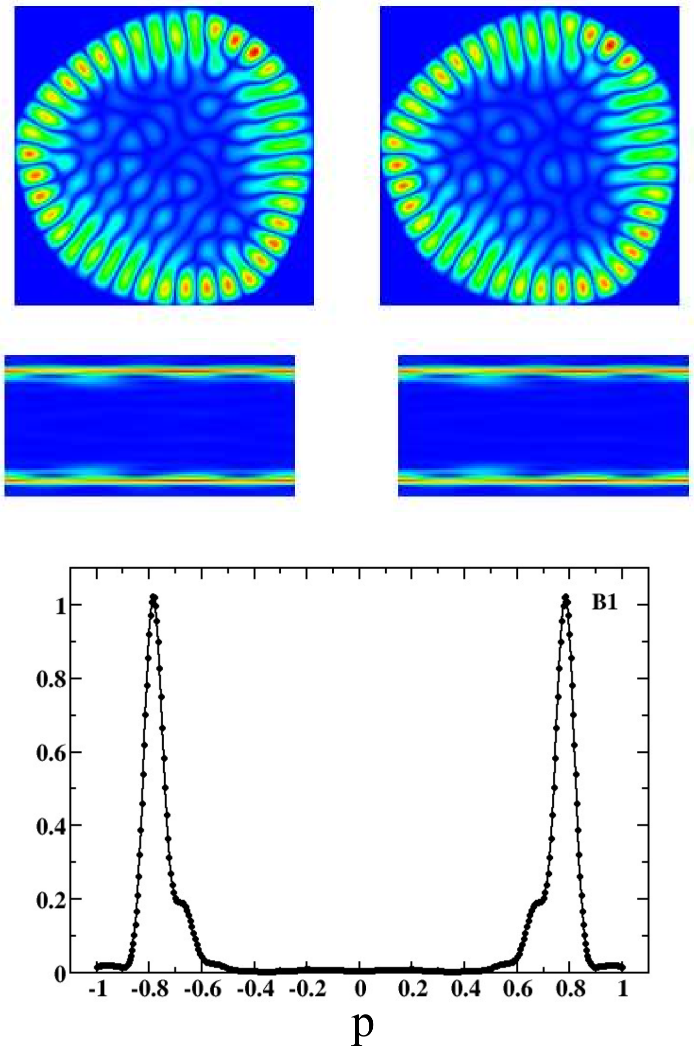

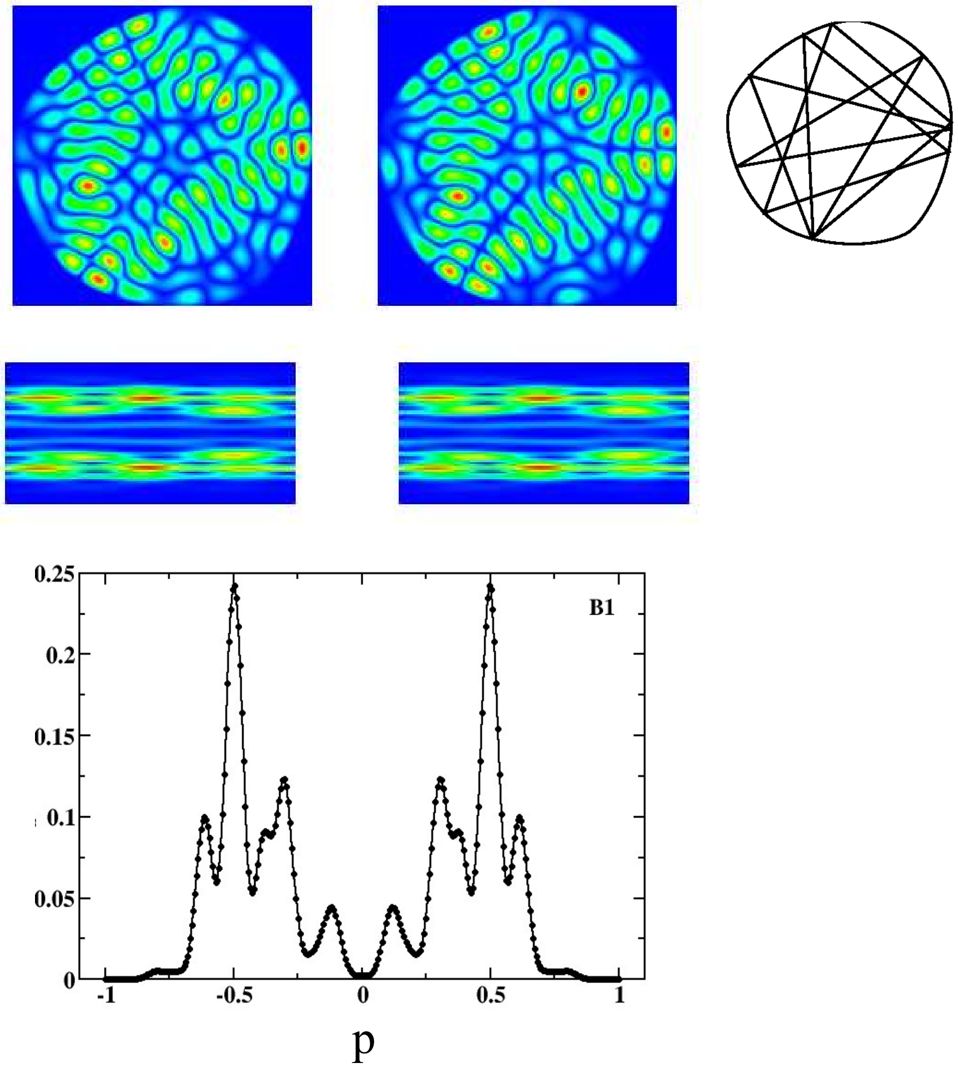

Regular Islands in Chaotic Sea of PSOS

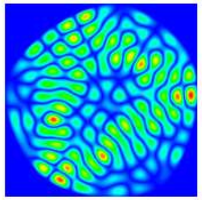

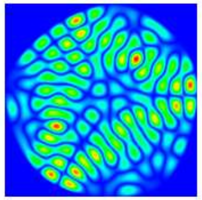

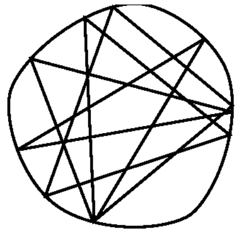

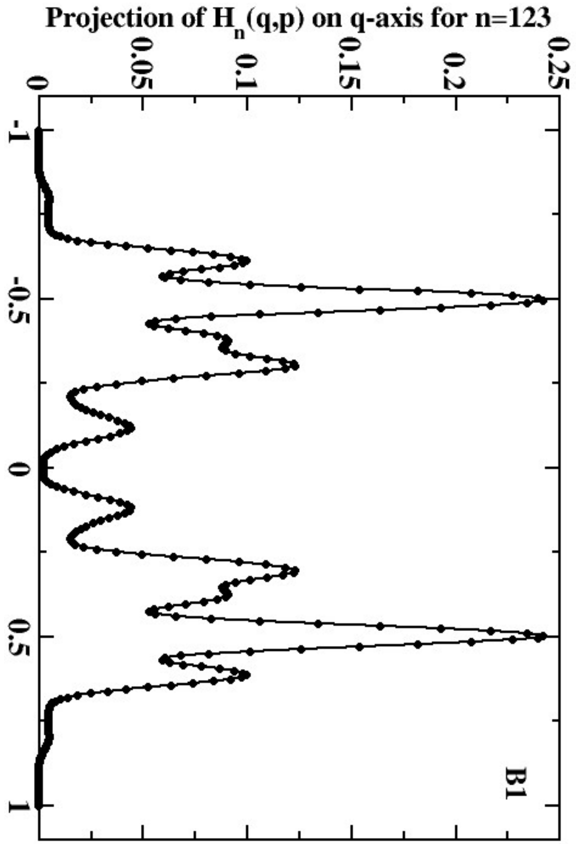

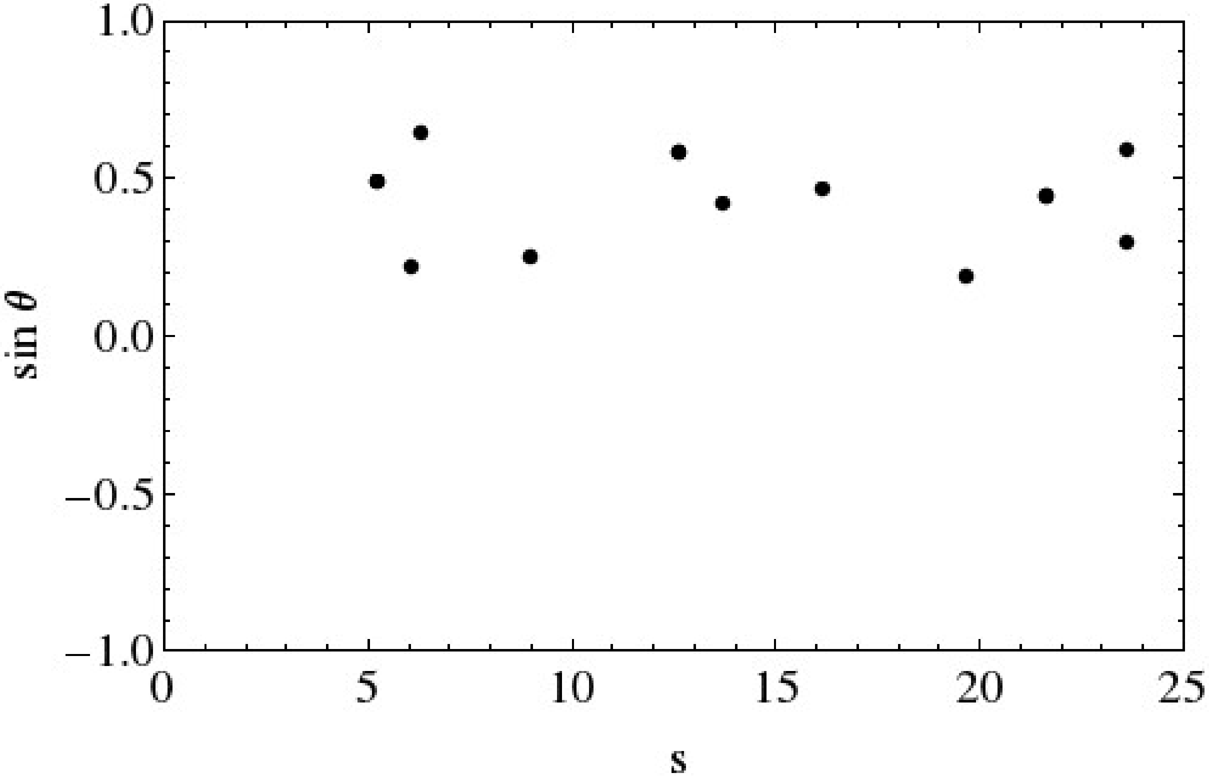

Splitting of the Doublett Partners

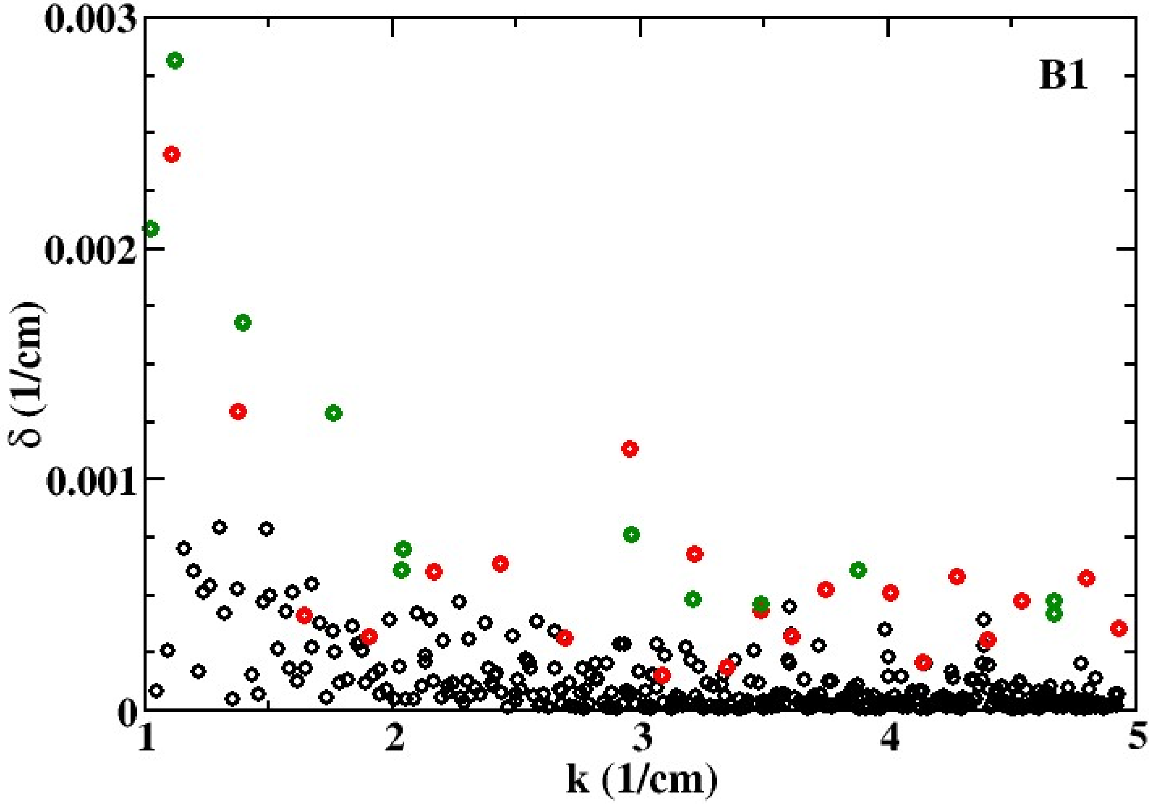

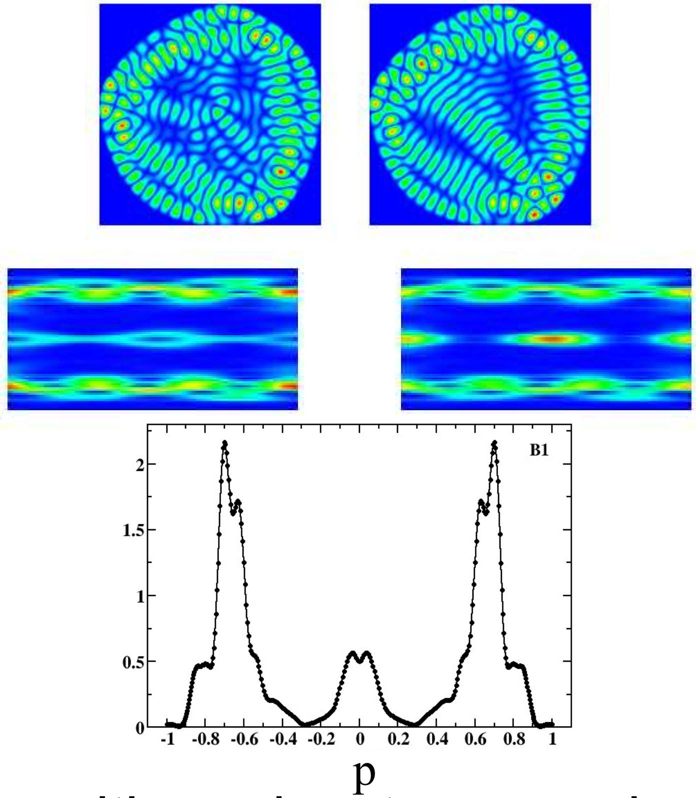

- Red and green circles mark ‘hybrid modes’ modes with peaks at zero and whispering gallery modes
- Husimi functions of pairs with large splittings all exhibit a maximum around diameter orbit → confirms assumption of tunneling via $p=0$ modes

RMT Model for the Spectral Properties

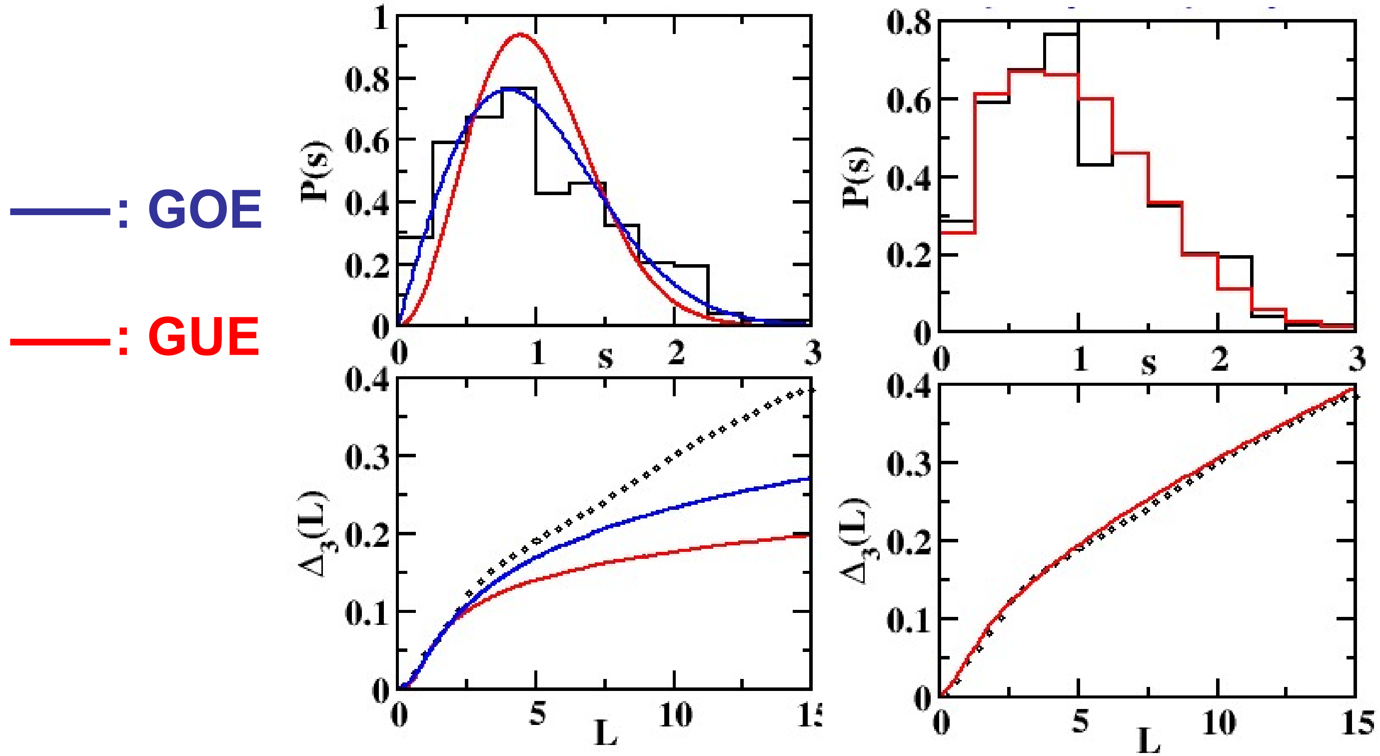

$$H^{mixed} = \begin{pmatrix} H & d_0\tau_1 V_1^\dagger \\ d_0\tau_1 V_1 & D_1 \end{pmatrix}$$

- Prediction: Due to unidirectionality the statistics is of GUE type
- But: The classical dynamics is mixed regular / chaotic in each half of PSOS
- V_1 couples H (chaotic dynamics) to D_1 (regular dynamics) with the coupling τ_1 measured in units of mean spacing d_0

Splitting-Weighted Density of States

S. Creagh, N. Whelan, PRL77 (1996)

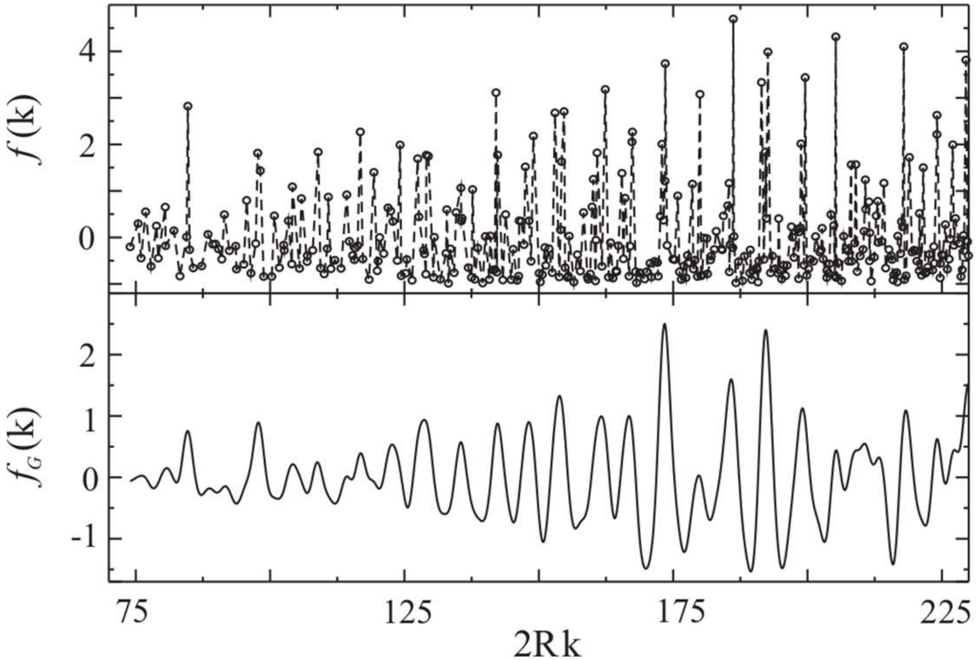

- Splitting-weighted density of states: $f(k) = \sum_n \left(\frac{\delta_n}{\langle \delta \rangle} - 1 \right) \delta(k - k_n)$
- Average with a Gaussian: $f_G(k) = \frac{1}{\sqrt{2\pi}\sigma} \int_0^\infty \mathrm{d}K\, f(K) e^{-\frac{(k-K)^2}{2\sigma^2}}$
- Large splittings recur periodically

Fourier Transform of Splitting-Weighted Density of States

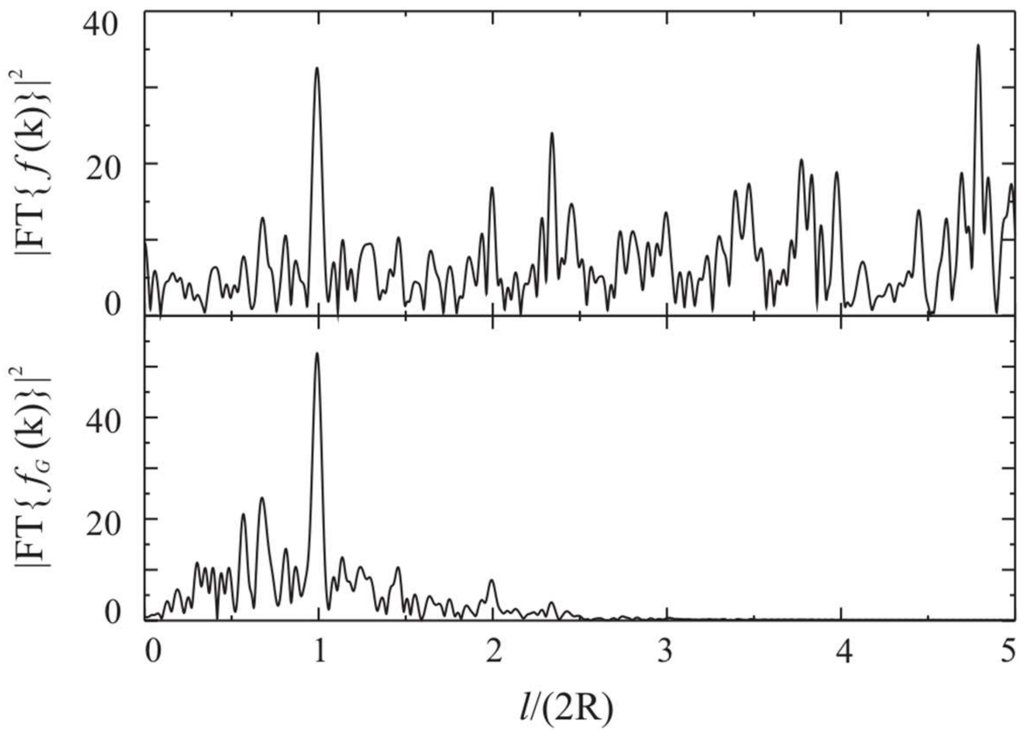

- Period corresponds to length of the billiard diameter
- Corroborates that tunneling is enhanced for states that are localized around the diameter orbits

Tunneling Model for Splitting Distribution

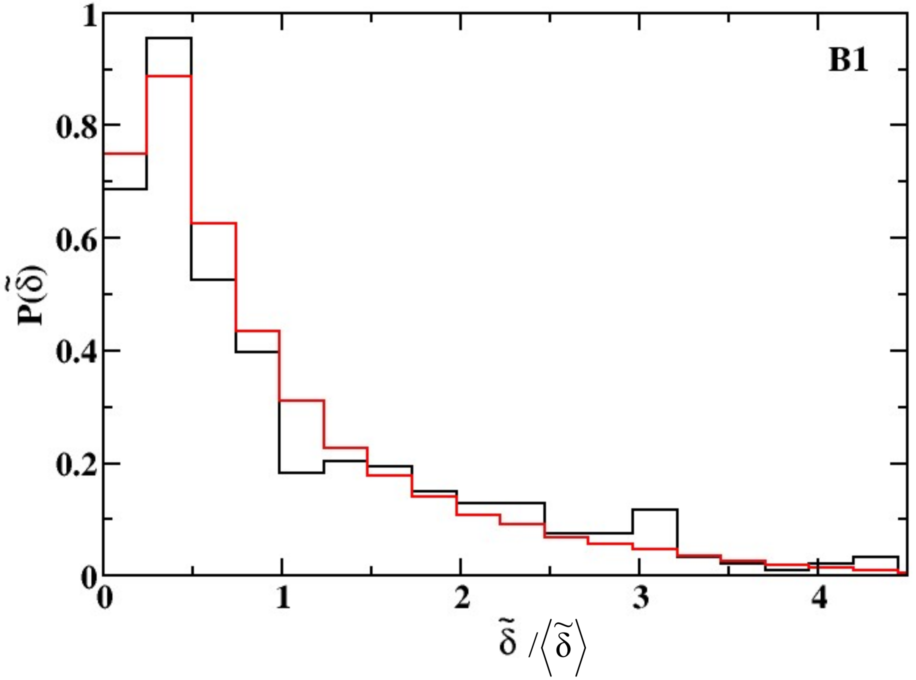

- RMT model: $$H^{splitting} = \begin{pmatrix} H^{mixed} & d\tau_2 V_2^\dagger & 0 \\ d\tau_2 V_2 & D_0 & d\tau_2 \tilde{V}_2^\star \\ 0 & d\tau_2 \tilde{V}_2^T & H^{*mixed} \end{pmatrix}$$

- Tunneling: V_2 couples H^{mixed} ($p>0$) with $(H^{mixed})^*$ ($p<0$) via D_0 (regular region around $p=0$) with coupling strength τ_2 measured in units of mean spacing d

Truncated Cauchy Distribution

F. Leyvraz, D. Ullmo, JPA 29 (1996)

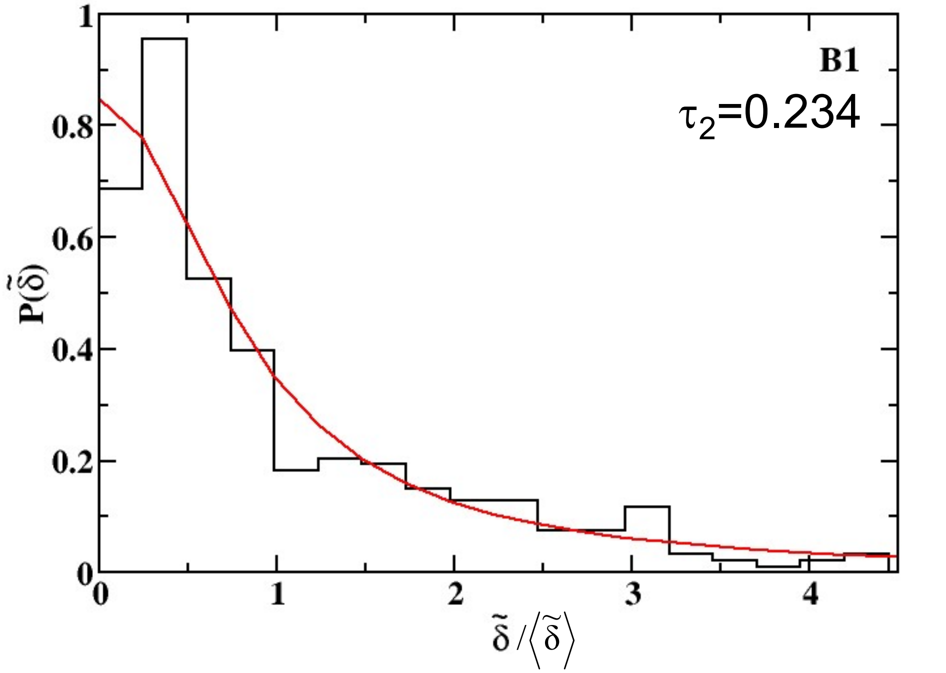

- Truncated Cauchy distribution

$$P(\tilde{\delta}) = \frac{2}{\pi}\frac{2\sqrt{\pi}\tau_2}{\tilde{\delta}^2 + 4\pi\tau_2^2} \quad \text{for} \quad \tilde{\delta} \leq \tau_2$$

- Fit to experimental splitting distribution yields approximately the same values for tunneling matrix element τ_2 as the RMT model for tunneling

PSM of 3 Limaçon Billiards
(Mixed integrable / chaotic dynamics)

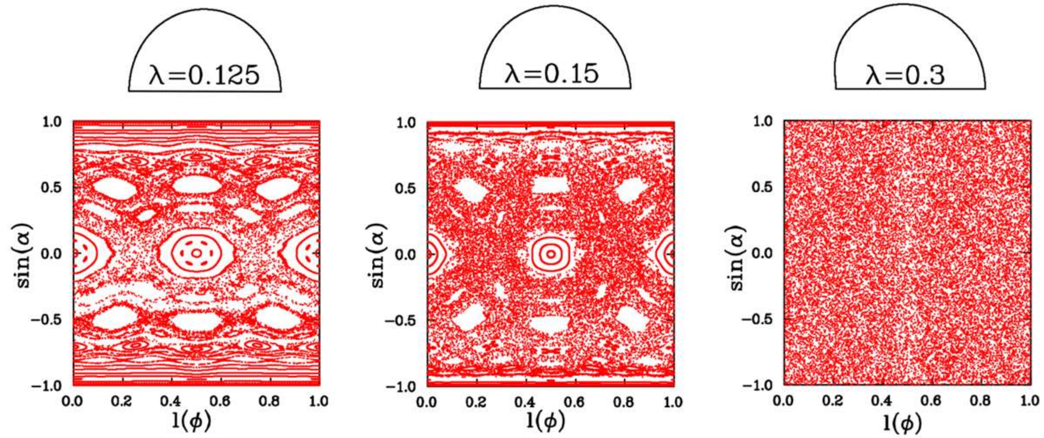

$$r(\varphi) = 1 + \lambda^2 + 2\lambda\cos\varphi$$

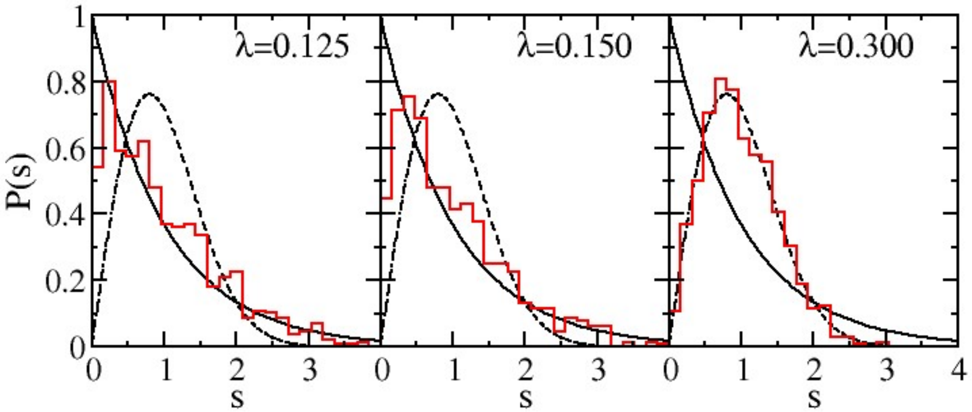

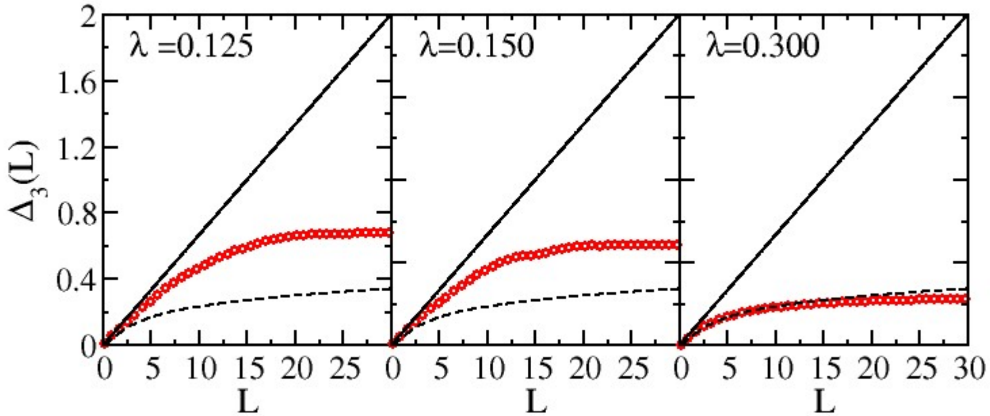

- The spectral properties change from Poisson and GOE with increasing λ / chaoticity

Fluctuating Part of the Integrated Resonance Density of a ¼ Stadium

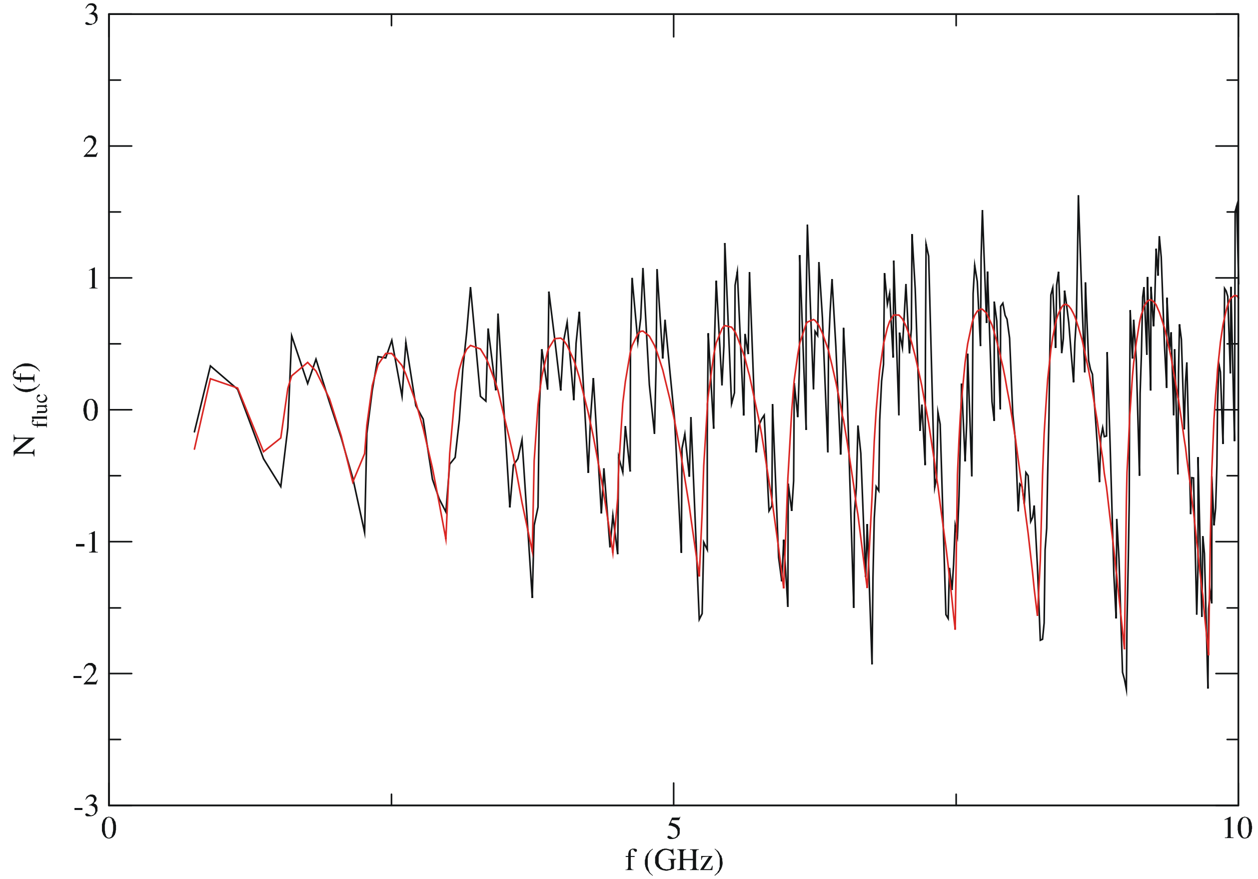

$$N(f) - N_{Weyl}(f) = N^{g.}_{fluc}(f)$$

$$\boxed{+N^{n.g.}_{osc}(f)}$$

- Non-generic orbits: `Bouncing Ball Orbits´

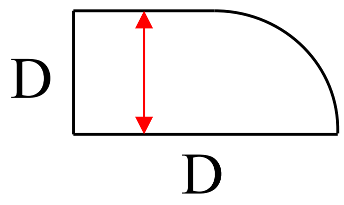

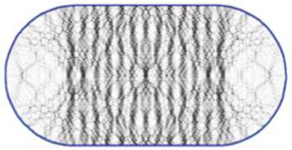

$$N^{n.g.}_{osc}(f) = \frac{a}{2\pi r}\sqrt{2\frac{fr}{c}}\sum_{m=1}^{\infty} m^{-3/2}\cos\left(4\pi m\frac{fr}{c} - \frac{3\pi}{4}\right)$$

[Sieber et al. JPA 26, 6217 (1993)]

Spectral Properties of a ¼ Stadium

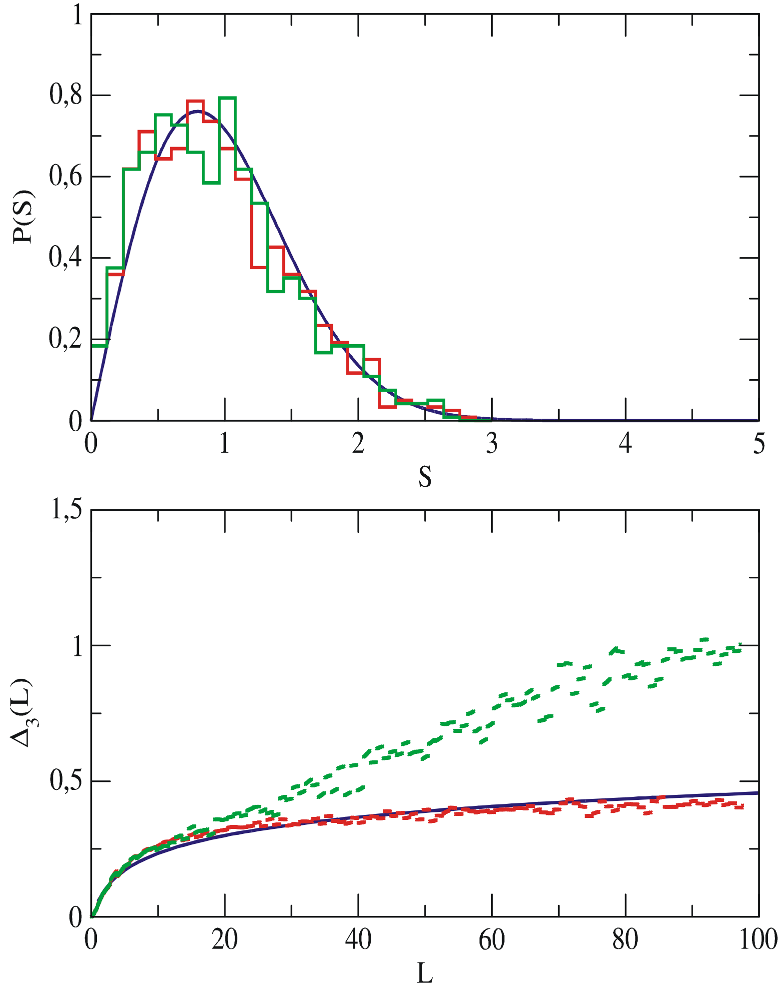

~1600 eigenfrequencies

- $e_i = N_{Weyl}(f_i)$
- $e_i = N_{Weyl}(f_i) + N_{osc}^{n.g.}(f_i)$

Fully Chaotic Tilted Stadium Billiard

- Tilted stadium (Primack + Smilansky, 1994)

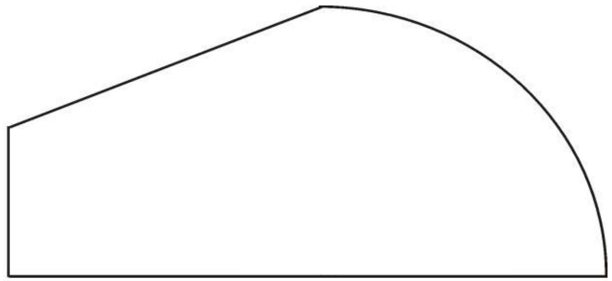

- 690 eigenvalues of quantum billiard were obtained from the resonance spectra with the harmonic inversion method

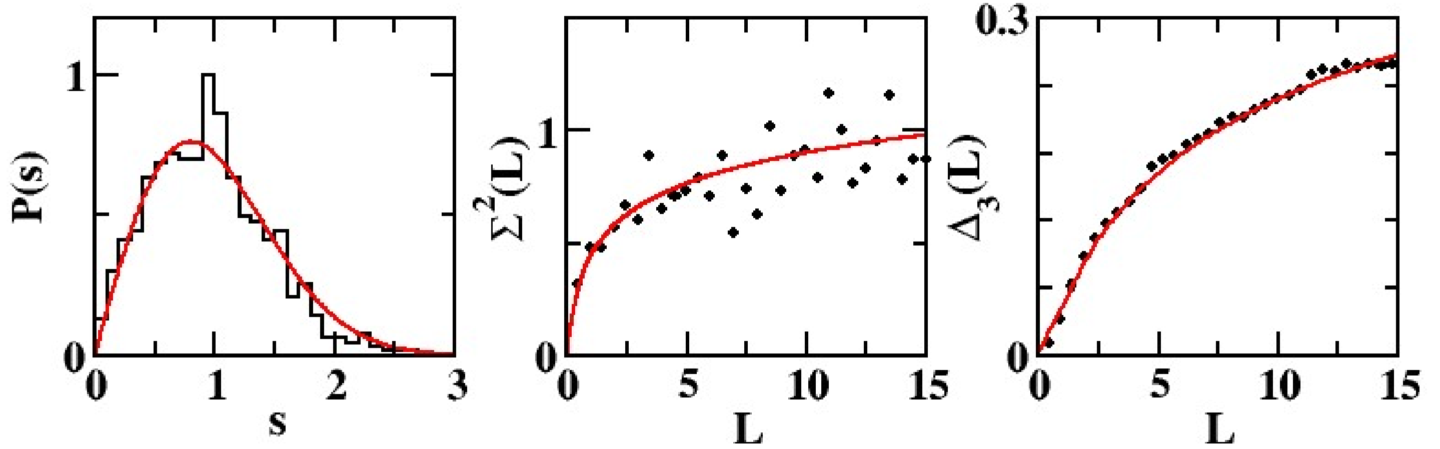

~800 eigenfrequencies

Quantum Graphs

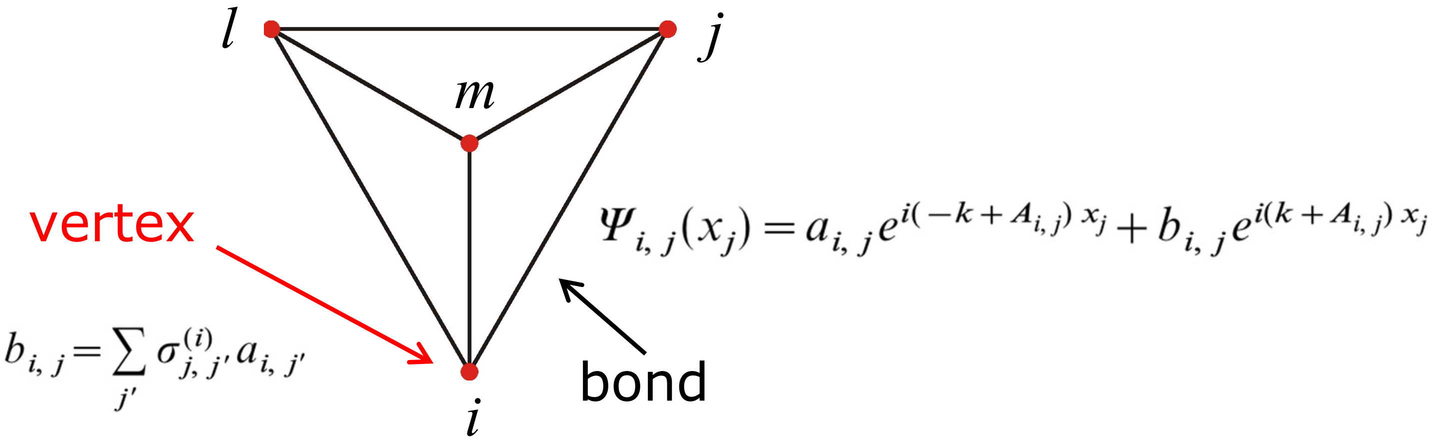

- Wave function on the bond connecting vertices i and j

$$\left(-i\frac{d}{dx} - A_{i,j}\right)^2 \Psi_{i,j}(x) = k^2 \Psi_{i,j}(x)$$

- The „magnetic vector potential" $A_{i,j}$ with $Re(A_{i,j}) \neq 0$ and $A_{i,j}=-A_{j,i}$ induces violation of time-reversal invariance
- For incommensurate bond lengths the wave dynamics is chaotic or Poisson depending on the boundary conditions at the vertices

→ graphs serve as a model system to study aspects of quantum chaos

Characteristics of Quantum Graphs

- Connectivity matrix element for vertices i and j

$$C_{i,j} = C_{j,i} = \begin{cases} 1 & \text{if } i, j \text{ are connected} \\ 0 & \text{otherwise} \end{cases}$$

- Continuity: $\Psi_{i,j}(0) = \varphi_i, \Psi_{i,j}(L_{i,j}) = \varphi_j$ for $i < j, C_{i,j} \neq 0$
- Current conservation:

$$\sum_{j<i} C_{i,j}\left(iA_{j,i} - \frac{d}{dx}\right)\Psi_{j,i}(x)\Big|_{x=L_{i,j}} + \sum_{j>i} C_{i,j}\left(-iA_{i,j} + \frac{d}{dx}\right)\Psi_{i,j}(x)\Big|_{x=0} = \lambda_i \varphi_i$$

- Vertex S-matrix: $\sigma^{(i)}_{ji,im} = \left(-\delta_{j,m} + \frac{1}{v_i}\left[1 + \frac{1 - i\Lambda_i}{\sqrt{1+\Lambda_i^2}}\right]\right) C_{ij}C_{im} \qquad \Lambda_i = \frac{\lambda_i}{v_i k}$
- Dirichlet boundary condition at vertex i corresponds to $\lambda_i \rightarrow \infty \Rightarrow$ Poisson

$$\sigma^{(i)}_{j,j'} = -\delta_{j,j'}$$

- Neumann boundary condition at vertex i corresponds to $\lambda_i = 0 \Rightarrow$ GEs apply

$$\sigma^{(i)}_{j,j'} = -\delta_{j,j'} + (2/v_i)$$

v_i: valency

Spectrum of Quantum Graphs

T. Kottos et al., Ann. Phys. 274, 76 (1999)

- Wave function on bond (i,j) with length $L_{i,j}$

$$\Psi_{i,j} = \frac{e^{iA_{i,j}x}}{\sin kL_{i,j}} \left(\varphi_i \sin[k(L_{i,j} - x)] + \varphi_j e^{-iA_{i,j}L_{i,j}} \sin kx\right) C_{i,j}, \qquad i < j.$$

- Current conservation yields the homogeneous set of linear equations

$$\hat{h}(k)\vec{\varphi} = \vec{0}$$

- Fulfilled for discrete values of k that solve the equation

$$\det \hat{h}(k) = 0$$

- Non-trivial solution:

with

$$h_{ij}(k) = \begin{cases} -\sum_{m \neq i} \cos(kL_{im}) \frac{C_{im}}{\sin(kL_{im})} & , i = j \\ C_{ij} e^{-iA_{ij}L_{ij} - i\phi_{ij}} \left[\sin(kL_{ij})\right]^{-1} & , i \neq j \end{cases}$$

Weyl formula:

$$\overline{N}\left(k = \sqrt{E}\right) = N^{Weyl}(k) = \frac{L^{tot}}{\pi} k + const.$$

Scattering Matrix for Open Quantum Graphs

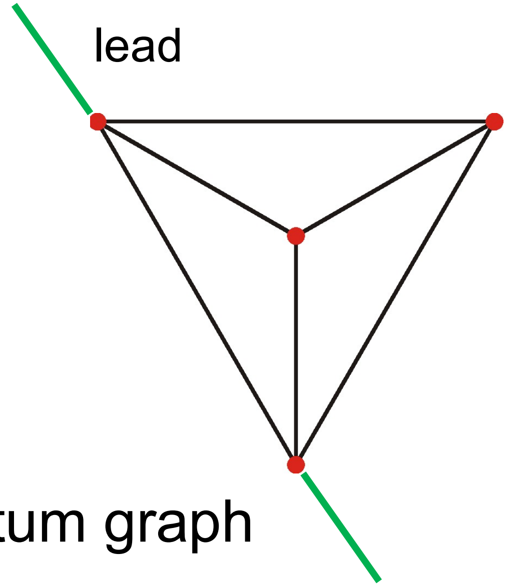

- The quantum graph is turned into a scattering system by attaching leads to it that extend to infinity
- (M×M)-dimensional scattering matrix:

$$\hat{S}_{\mathcal{V}}(k) = \mathbb{1}_{\tilde{M}} - 2i\hat{W}^T \left[\hat{h}(k) + \frac{i}{2}\hat{W}\hat{W}^T\right]^{-1} \hat{W}$$

M = # leads, $\mathcal{V}$ = # vertices

- (M×$\mathcal{V}$)-dimensional matrix $\hat{W}$ describes coupling of quantum graph to the exterior through the leads
- Time-reversal invariance: $\hat{T}\hat{S}_{\mathcal{V}}\hat{T}^{-1} = \hat{S}_{\mathcal{V}}^{\dagger} = \hat{S}_{\mathcal{V}}^{-1}$
- An exact semiclassical approximation (trace formula) has been derived for the fluctuating part of the spectral density

$$\rho^{fluc}(k) = \frac{1}{\pi} \sum_{p\in\mathcal{P}_n} \frac{l_p \cos\left(r\left[kl_p + \pi\mu_p\right]\right)}{e^{r(n_p\gamma_p/2)}} \quad \text{with} \quad e^{-n_p\gamma_p/2} = \prod_{s=1}^{\mu_p}\left|\left(1-\frac{2}{v_s}\right)\right|\prod_{s=1}^{n_p-\mu_p}\left|\frac{2}{v_s}\right|$$

Spectral Properties of Graphs with Preserved T Invariance (GOE)

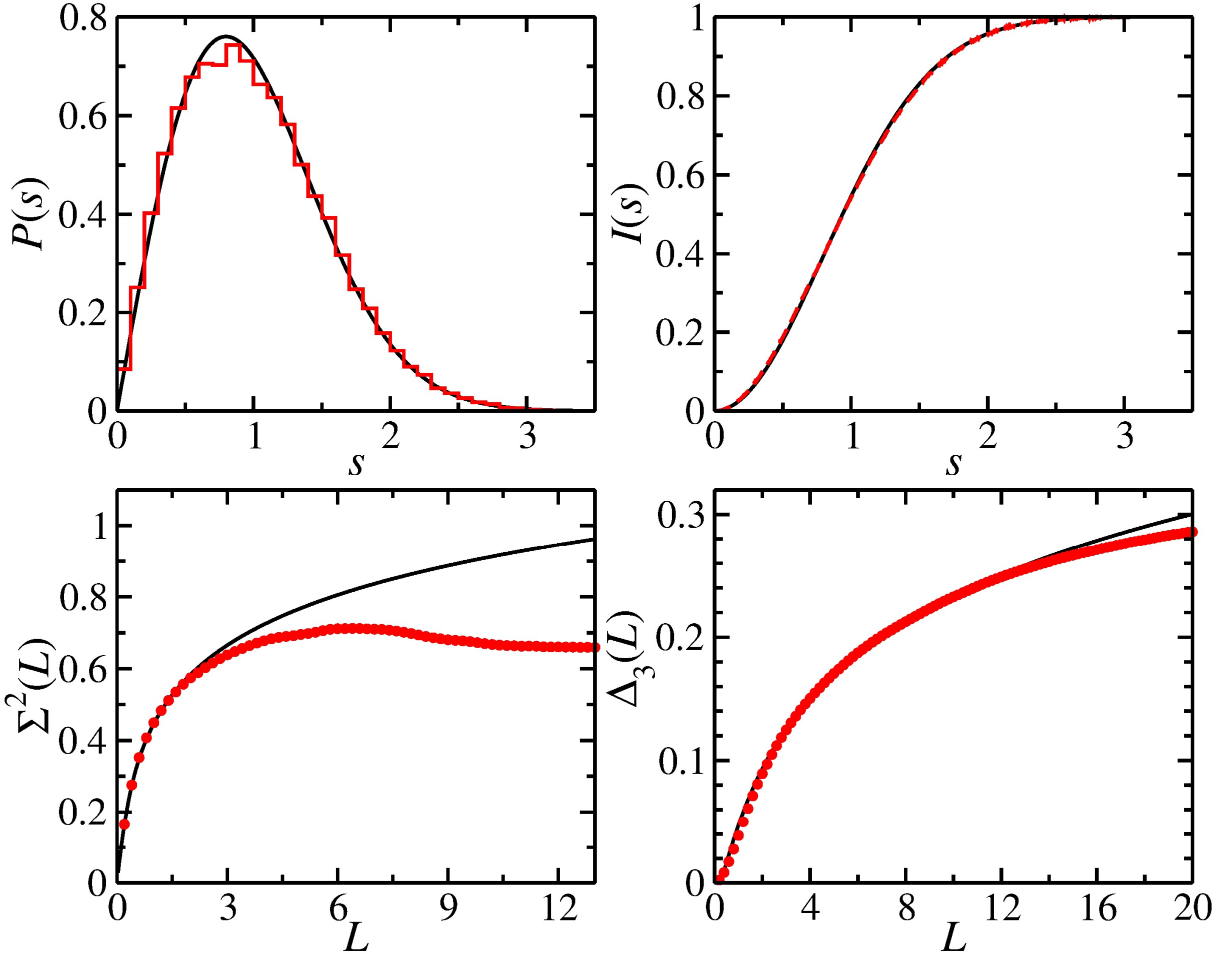

- The long-range spectral fluctuations deviate from the GOE curves for L>3 (8)

Fluctuating Part of the Integrated Spectral Density of the Computed Eigenvalues

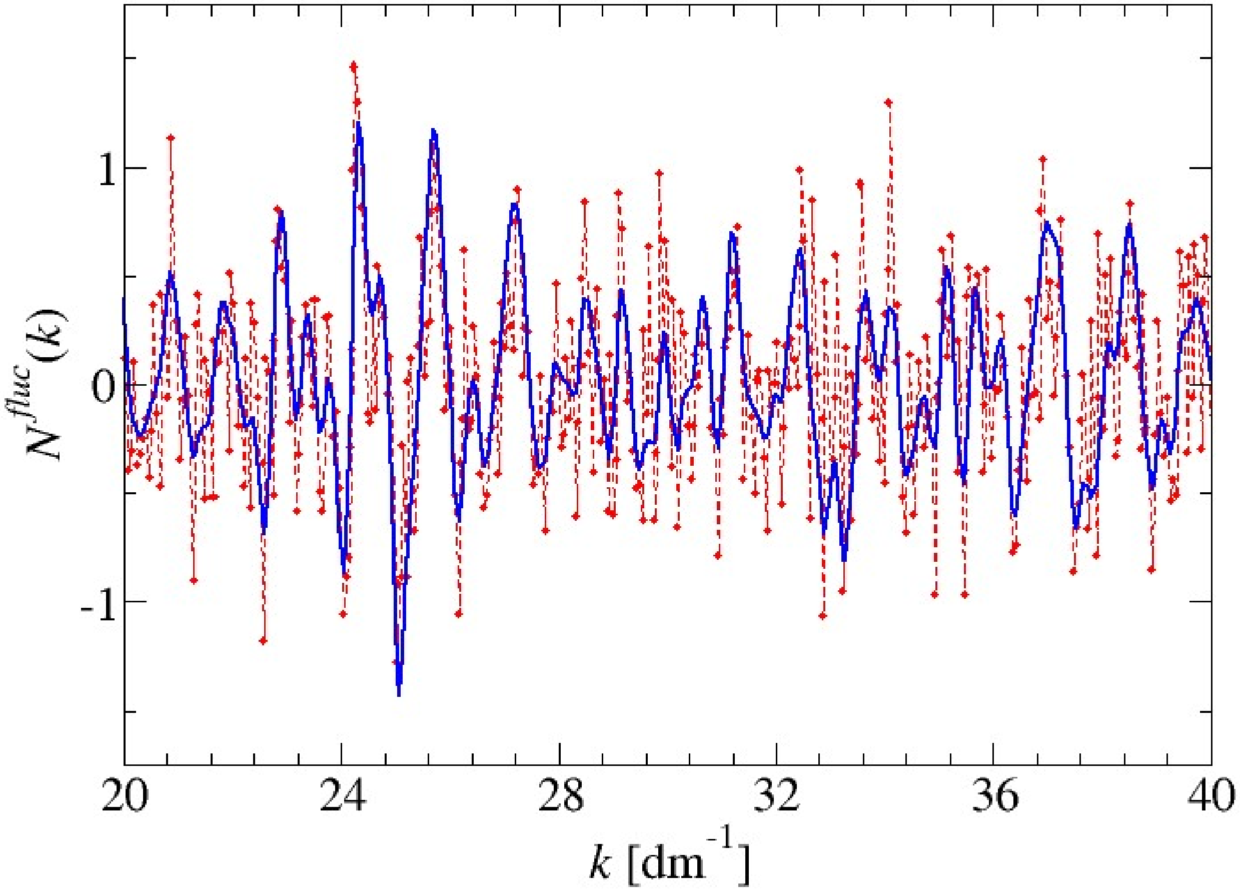

: numerics

: smoothed $N^{fluc}(k)$

- Fluctuating part of the integrated spectral density exhibits slow oscillations

$\rightarrow$ We applied the exact trace formula for quantum graphs to find their origin (a general procedure to identify nonuniversal effects)

Trace Formula for Quantum Graphs

T. Kottos et al., Ann. Phys. 274, 76 (1999)

- Take into account only orbits confined to a bond, bouncing back and forth between the two vertices

$$\rho^{fluc}(k) = \frac{1}{\pi}\sum_{r}\sum_{i,j}\left(\frac{9}{25}\right)^{r} 2L_{i,j}\cos\left(rk2L_{i,j}\right)$$

$$i \quad \leftrightarrow \quad j$$

- Orbits confined to a bond do not sense the chaoticity of the dynamics arising due to the joint effect of the scattering at all vertices

$\rightarrow$ exhibit nonuniversal features

- Such orbits are absent in unidirectional graphs

- To demonstrate the dominance of these orbits in the spectra we compared results for $N^{fluc}(k)$ and length spectra

Fluctuating Part of Integrated Spectral Density
Dietz et al., PRE 95, 052202 (2017)

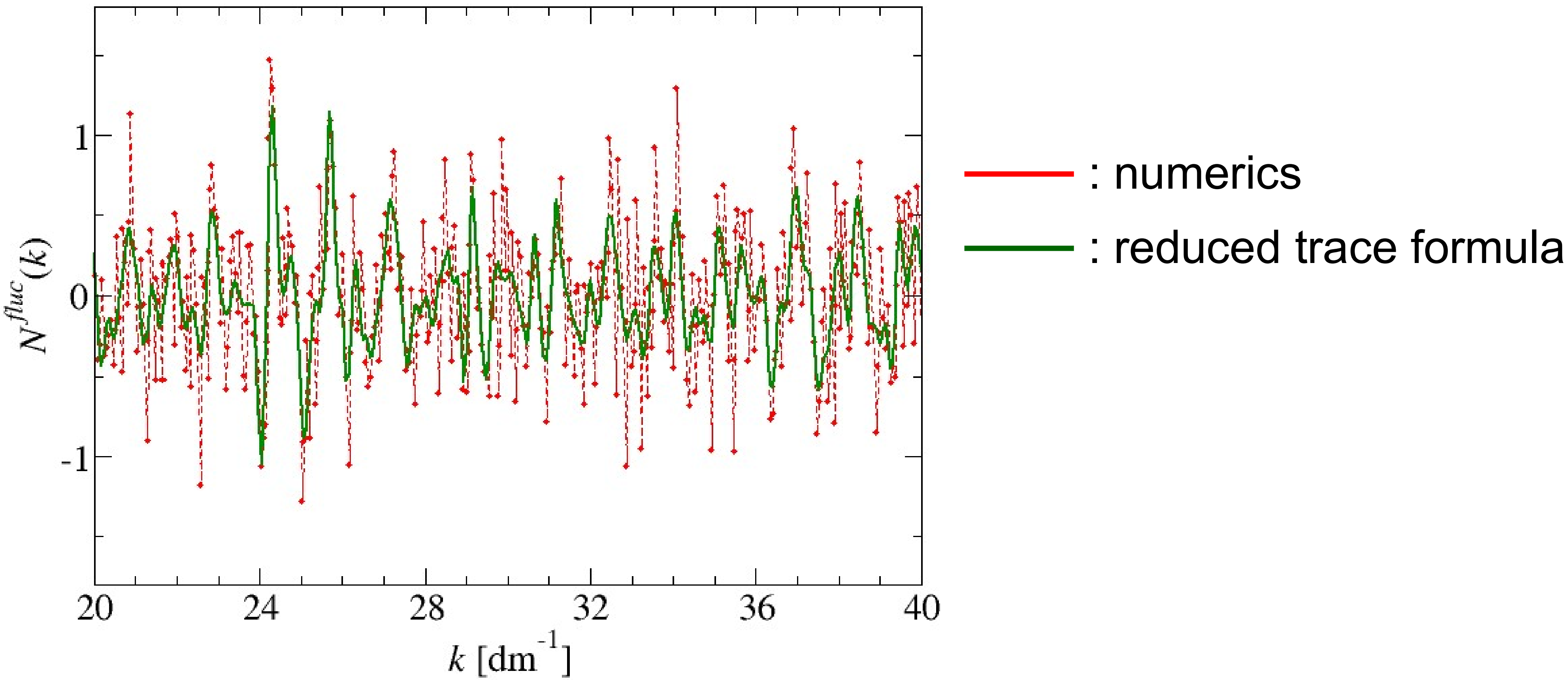

- The slow oscillations are well described by the integrated semiclassical trace formula taking into account only orbits that are confined to individual bonds

Comparison of a Numerical & Semiclassical Length Spectrum

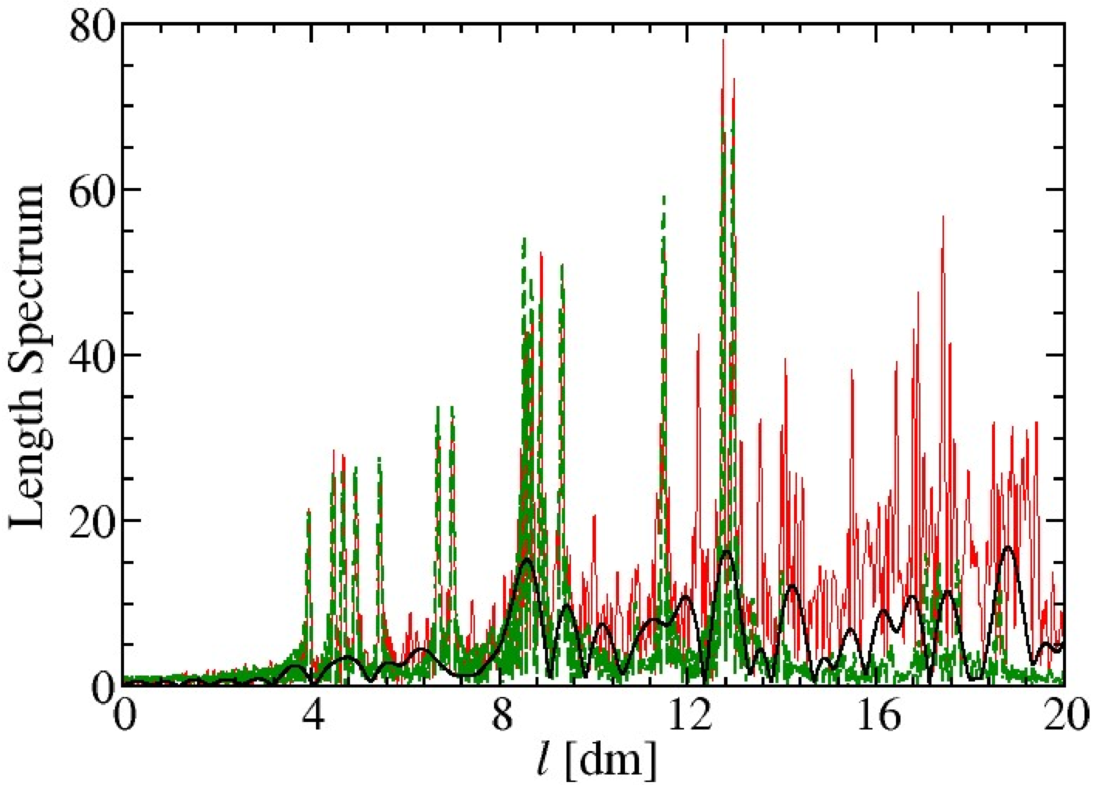

: experiment

: numerics

: semiclassical length spectrum

Length spectrum

$$\left|\tilde{\rho}(l)\right| = \left|\int_0^{k_{max}} dk e^{ikl} \rho^{fluc}(k)\right|$$

- For the shortest lengths, the experimental and the numerical length spectra are well described by the semiclassical one including only periodic orbits confined to individual bonds

$\rightarrow$ Backscattering at the joints of the quantum graphs is nonnegligible thus leading to nonuniversal features in spectral properties

Threefold way

- Quantum systems with violated time-reversal invariance
- Hamiltonian (unitary universality class):

$$\hat{H} = \hat{H}^{\dagger}.$$

- Quantum Systems with integer spin and preserved time-reversal invariance
- Time-reversal operator

$$\hat{T} = \mathcal{C} \quad \hat{T}^2 = 1$$

- Hamiltonian (orthogonal universality class):

$$\hat{T}\hat{H}\hat{T}^{-1} = \hat{H} \quad \hat{H} = \hat{H}^{T}$$

- Quantum systems with 1/2-integer spin and preserved time-reversal invariance belong to the symplectic universality class

Hamiltonian with Symplectic Symmetry (GSE)

- Time-reversal operator of spin-1/2 systems $\hat{T} = \hat{Y}\mathcal{C},\, \hat{Y} = \begin{pmatrix} \hat{0}_N & -\mathbb{1}_N \\ \mathbb{1}_N & \hat{0}_N \end{pmatrix}$
- Time-reversal invariance $\hat{T}\hat{H}\hat{T}^{-1} = \hat{H}$
- Hermiticity implies that $\hat{H} = \hat{H}^\dagger$ is symplectic

$$\hat{H} = \hat{Y}\hat{H}^T\hat{Y}^T$$

- The eigenvalues are Kramer's degenerate $\hat{T}^2 = -1 \;\Rightarrow\; \langle\psi|\hat{T}\psi\rangle = 0$
- Define basis $\mathcal{B} = \{|1\rangle, |2\rangle \ldots, |N\rangle, |\hat{T}1\rangle, |\hat{T}2\rangle, \ldots, |\hat{T}N\rangle\}$
- Symplectic Hamiltonian $\hat{H} = \begin{pmatrix} \hat{H}_0 & \hat{V} \\ -\hat{V}^* & \hat{H}_0^* \end{pmatrix},\, \hat{H}_0 = \hat{H}_0^\dagger,\, \hat{V} = -\hat{V}^T$

Quantum Graph with Symplectic Symmetry

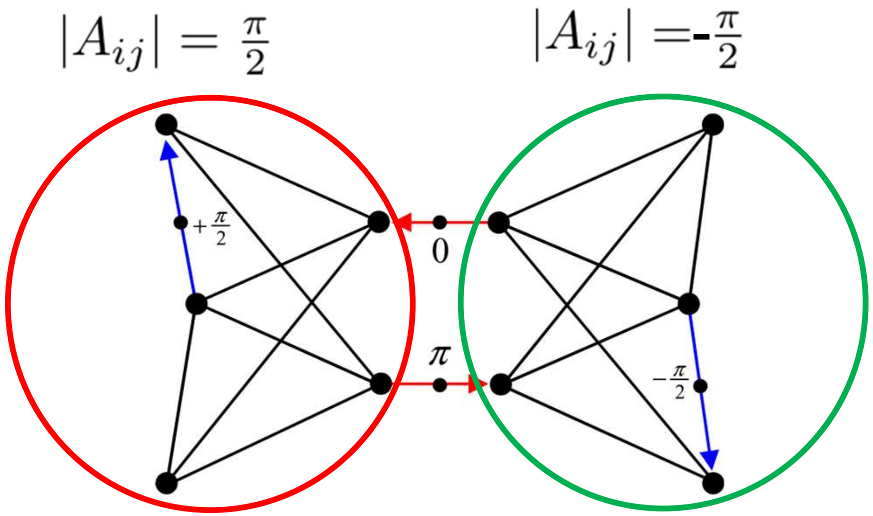

$$\hat{H} = \begin{pmatrix} \hat{H}_0 & \hat{V} \\ -\hat{V}^* & \hat{H}_0^* \end{pmatrix}, \hat{H}_0 = \hat{H}_0^\dagger, \hat{V} = -\hat{V}^T$$

- Introduced by [A. Rehemanjiang et al. Phys. Rev. Lett. 117, 064101 (2016)]
- Graphs are identical except for a phase of $\pm\pi/2$
- Time-reversal invariance is induced by a magnetic vector potential $A_{i,j} = \pm\pi/2$ at two corresponding bonds\
- Coupling is realized with two bonds of same length and a relative phase of π

Spectral Properties of Graphs with Violated *T* Invariance and with Symplectic Symmetry

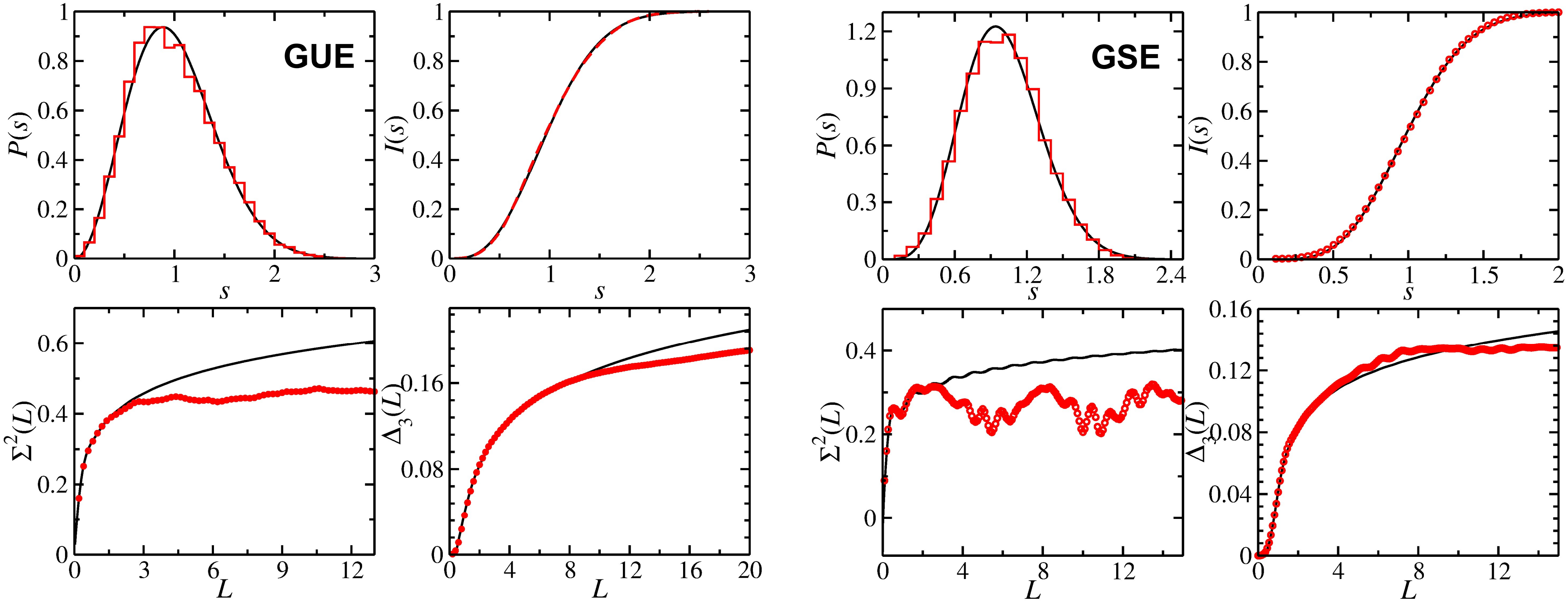

- The long-range spectral fluctuations deviate from the GUE / GSE curves for L>3 (8)
- Origin: backscattering at the vertices

Level Dynamics of GUE and GSE Graph

J. Lu et al., PRE 102, 022309 (2020)

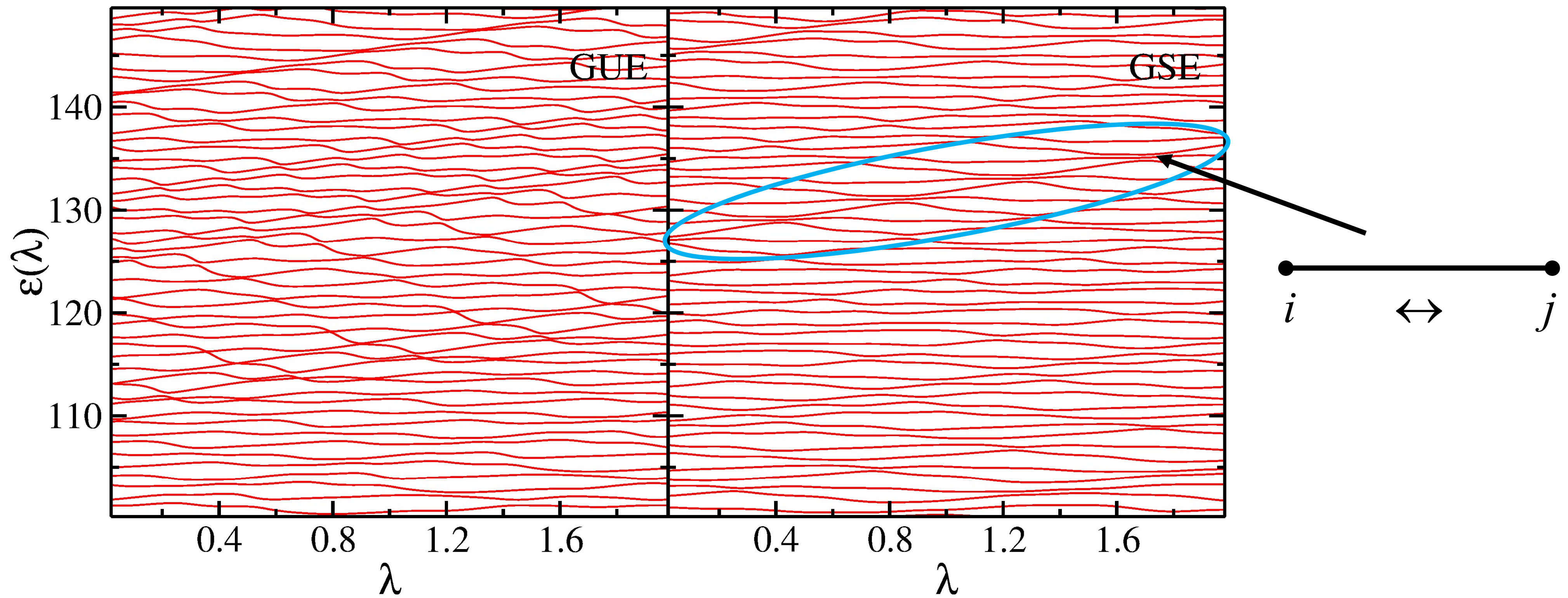

- The lengths of two pairs of corresponding bonds is varied while keeping the spectral density $\rho(k)$ fixed.
- The stripes of constant slopes correspond to trapped modes

Curvature Distributions

- Before extraction of nonuniversal contributions

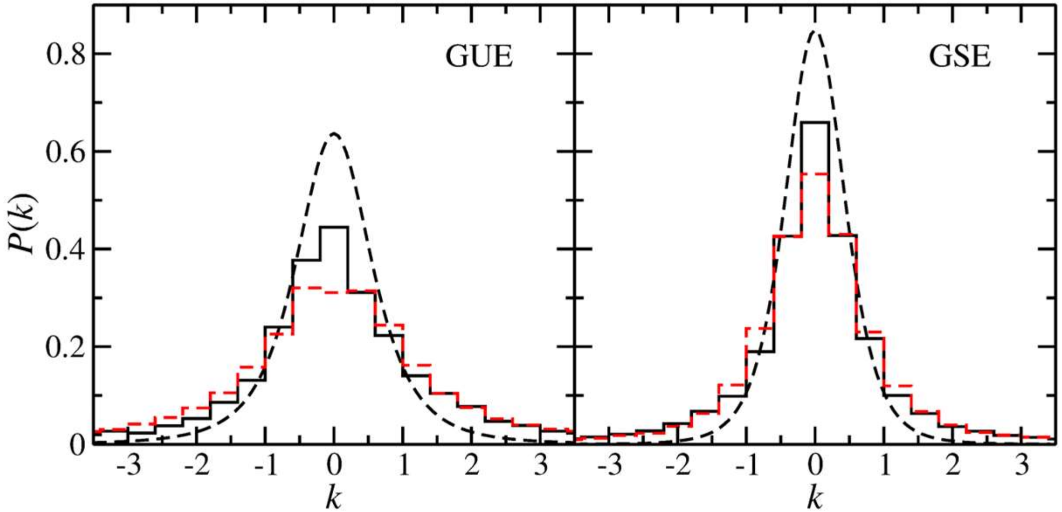

- After extraction of nonuniversal contributions

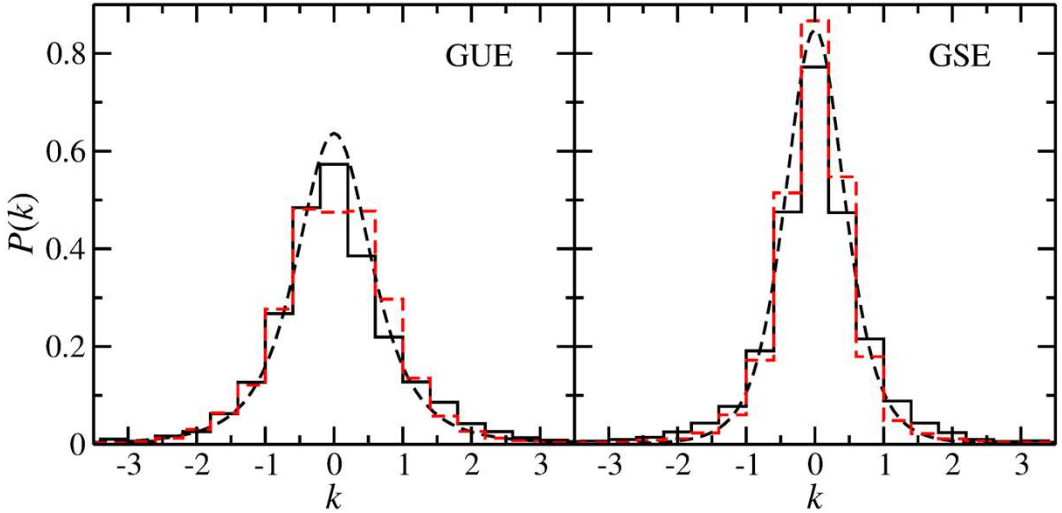

Avoided Crossing Distributions

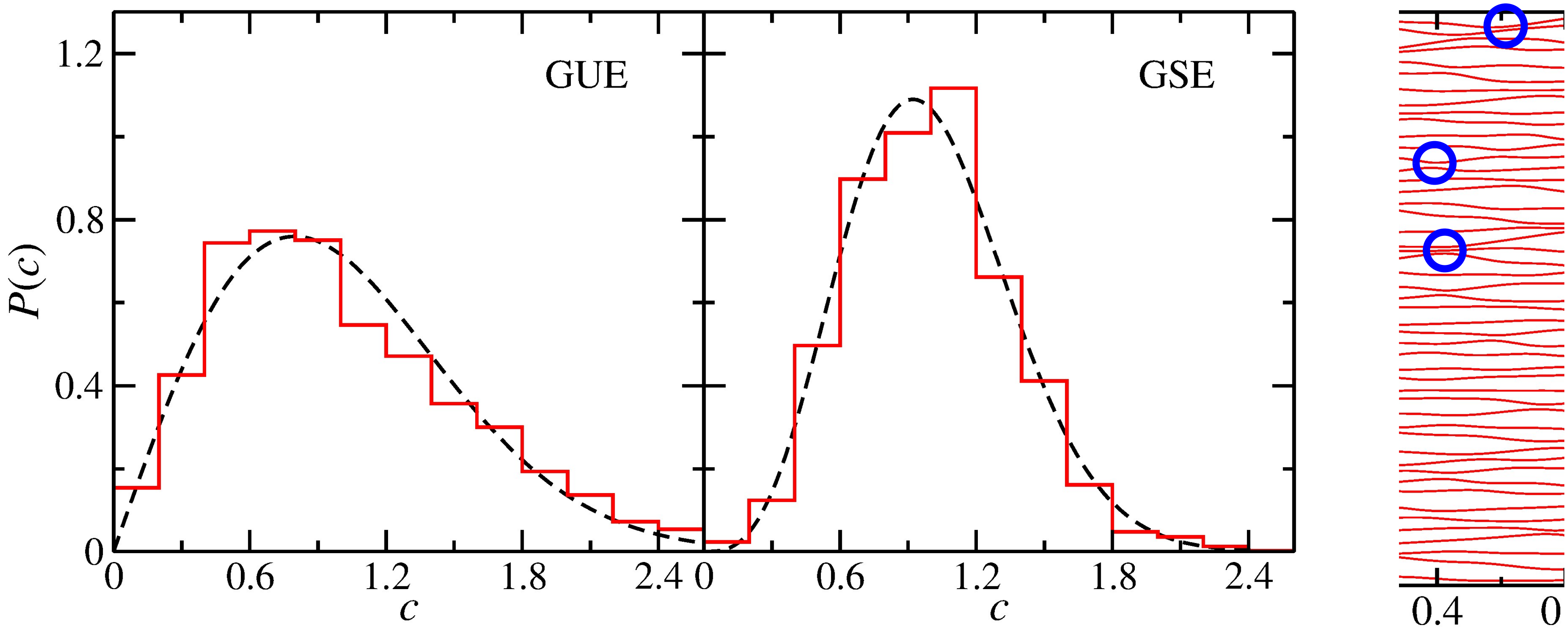

- Distribution of the distances between adjacent levels at lengths of closest encounter

Thank you

for

your attention

RMT Model for Poisson to GOE Transitions

V.K.B. Kota, Lecture Notes in Physics 884, Chapter 3.2

- Ansatz for random matrices with spectral properties intermediate between Poisson and GOE statistics

$$H(\lambda) = \frac{H_0 + \lambda H_1}{\sqrt{1+\lambda^2}} \qquad \begin{array}{ll} \lambda = 0: & \text{Poisson} \\ \lambda \to \infty: & \text{GOE} \end{array}$$

- H_0: diagonal matrix containing random Poissonian numbers
- H_1: random matrix from the GOE
- Variances of matrix elements were chosen such, that the lengths of the level sequences of H_0 and H_1 coincided
- Spectral properties are indistinguishable from GOE for $\lambda \approx 1\text{-}2$
- Wigner-like approximation for the NNSD in terms of the $I_0(x)$ Bessel function and the $U(a,b,x)$ Kummer function [G. Lenz & F. Haake, PRL **67**, 1 (1991)]

$$P_{P\to GOE}(s,\lambda) = \frac{su(\lambda)^2}{\lambda}\exp\left[-u(\lambda)^2 s^2/4\lambda^2\right]\int_0^\infty d\xi e^{-\xi^2-2\xi\lambda} I_0\left[\xi\, s\, u(\lambda)/\lambda\right],\ u(\lambda) = \sqrt{\pi}U(-1/2,0,\lambda^2)$$